UNIVERSITY OF CALIFORNIA

Los Angeles

Quantum information through holography and applications

A dissertation submitted in partial satisfaction

of the requirements for the degree

Doctor of Philosophy in Physics

by

Andrea Trivella

2019

ABSTRACT OF THE DISSERTATION

Quantum information through holography and applications

by

Andrea Trivella

Doctor of Philosophy in Physics

University of California, Los Angeles, 2019

Professor Eric D'Hoker , Chair

In this dissertation we explore how some information theory quantities can be formulated holographycally and used to explore and characterize strongly interacting quantum field theories. In Chapter 1 we give a holographic formulation of the Quantum Information Metric, a quantity that measures the distance between two infinitesimally different quantum states. After giving the general prescription we illustrate its use in different examples and show how it reproduces the expected field theory results.

In Chapter 2 we explore another quantum information theory quantity that finds vast applications in holography: entanglement entropy. In particular we focus on the regularization of the entanglement entropy for holographic interface theories. The fact that globally well defined Fefferman-Graham coordinates are difficult to construct makes the regularization of the holographic theory challenging. We introduce a simple new cut-off procedure, which we call "double cut-off" regularization.

While the spirit of the first two chapters is to develop tools that can be used in studying quantum field theories holographically, in Chapters 3 and 4 we switch gears and explore a concrete example of holographic duality: we study type IIB Supergravity duals to 5 dimensional super-conformal field theories. In Chapter 3 we look at a class of bulk solutions without monodromy. The solutions exhibit mild singularities, which could potentially com-

plicate holographic applications. We use the relation of the entanglement entropy for a spherical entangling surface to the free energy of the field theory on the five sphere as a well-motivated benchmark to assess how problematic the singularities are. The holographic supergravity computations give well-defined results for both quantities and they satisfy the expected relations. This supports the interpretation of the solutions as holographic duals for 5d SCFTs and gives first quantitative indications for the nature of the dual SCFTs.

In chapter 4 we discuss bulk solutions that include punctures around which the supergravity fields have non-trivial $SL(2,\mathbb{R})$ monodromy. We show that punctures with infinitesimal monodromy match a probe 7-brane analysis using κ-symmetry and we construct families of solutions with fixed 5-brane charges and punctures with finite monodromy, corresponding to fully backreacted 7-branes. We compute the sphere partition functions of the dual 5d SCFTs and use the results to discuss concrete brane web interpretations of the supergravity solutions.

The dissertation of Andrea Trivella is approved.

Michael Gutperle

David Gieseker

Eric D'Hoker, Committee Chair

University of California, Los Angeles

2019

Contents

List of Figures

Acknowledgements

I would like to thank Eric D'Hoker, my advisor, for his mentorship and collaboration. I also want to thank Michael Gutperle and Christopher Uhlemann. Working on projects with them has been not only educational and enriching, but also a lot of fun.

Finally I would like to thank my parents, Marco e Maria Teresa, for teaching me that hard work and honesty will take you a long way, grazie.

Contribution of authors

Chapter 1 is based on [1] and [2], in collaboration with Dongsu Bak. Chapter 2 is based on [3], in collaboration with Michael Gutperle. Chapter 3 is based on [4], in collaboration with Michael Gutperle, Chrysostomos Marasinou and Christoph F. Uhlemann. Chapter 4 is based on [5], in collaboration with Michael Gutperle and Christoph F. Uhlemann.

Vita

2011	B.S. (Physics), Università Cattolica del Sacro Cuore, Brescia, Italy
2013	M.S. (Physics), Università Cattolica del Sacro Cuore, Brescia, Italy
2013 – 2019	Teaching Assistant, Department of Physics and Astronomy, UCLA

Publications

"Holographic Computations of the Quantum Information Metric,"
Trivella, A., Class. Quant. Grav. **34** (2017) no.10, 105003
DOI:10.1088/1361-6382/aa69a6 arXiv:1607.06519 [hep-th]

"Note on entanglement entropy and regularization in holographic interface theories,"
M. Gutperle and A. Trivella, Phys. Rev. D **95**, no. 6, 066009 (2017)
DOI:10.1103/PhysRevD.95.066009 arXiv:1611.07595 [hep-th]

"Entanglement entropy vs. free energy in IIB supergravity duals for 5d SCFTs,"
M. Gutperle, C. Marasinou, A. Trivella and C. F. Uhlemann, JHEP **1709**, 125 (2017)
DOI:10.1007/JHEP09(2017)125 arXiv:1705.01561 [hep-th]

"Quantum Information Metric on $\mathbb{R} \times S^{d-1}$,"
D. Bak and A. Trivella, JHEP **1709**, 086 (2017)
DOI:10.1007/JHEP09(2017)086 arXiv:1707.05366 [hep-th]

"Type IIB 7-branes in warped AdS_6: partition functions, brane webs and probe limit,"
M. Gutperle, A. Trivella and C. F. Uhlemann,, JHEP **1804**, 135 (2018)
DOI:10.1007/JHEP04(2018)135 arXiv:1802.07274 [hep-th]

Chapter 1

Holographic Computations of the Quantum Information Metric

Since the formulation of AdS/CFT correspondence there has been a great effort in trying to understand how gravity can emerge from the degrees of freedom of the dual field theory. In this context entanglement entropy has been a promising tool. Entanglement entropy has been extensively studied not only because it is an order parameter for quantum phase transitions [6], but because the celebrated proposal for the computation of holographic entanglement entropy [7] has given a geometric interpretation to a quantity that is intrinsically quantum mechanical. This geometric interpretation has helped in building further connections between the gauge and the gravity sides of the duality [8–10].

Due to the fact that entanglement entropy is hard to calculate theoretically and difficult to measure experimentally, it may be useful to find other quantum information quantities that could be understood holographically.

One quantity that has been recently explored is the Quantum Information Metric (QIM). It is defined on an infinite-dimensional space of all the deformations induced by all possible operators away from the unperturbed theory. The authors of [11] and [12] have focused only on deformations induced by a single marginal operator. In that particular case one can argue

that the QIM can be constructed from the on shell action of a Janus type solution [13]. Since this solution is generally not available the authors of [11] have suggested that the Janus solution could be replaced by a probe brane. This prescription is limited to the case of deformation induced by marginal operators, in addition it reproduces results only qualitatively and up to an order one constant.

In this chapter we present the results of [1, 2], where the QIM was obtained holographically using perturbative techniques: since the QIM measures the distance between two infinitesimally separated states this approach is natural. The study is limited to a change of state induced by deforming the Lagrangian of the theory by a conformal primary operator. From the bulk point of view this means that the scalar field dual to the operator that induces the deformation on the CFT side is going to be considered as a perturbative excitation of an unperturbed background (dual to the CFT state that we are deforming). This allows us to extend previous results to deformations induced by any primary scalar operators (not necessarily marginal) and to explore configurations in which the Janus solution is not available.

The chapter is organized as follows: We introduce the definition of QIM in section 1.1. In section 1.2, after defining the QIM for a CFT deformed by a primary operator of dimension $\Delta > d/2 + 1$, we give a holographic construction of this quantity. This extends the results available in the existing literature where the holographic computation was performed only in the case of a marginal deformation. In section 1.3 we put the CFT on a cylinder, we suggest a formula for the universal contribution of the QIM. In section 1.4 we relate the computation of the QIM for a marginal deformation on the cylinder to the computation of the free energy for an interface theory on a sphere. We conclude the chapter with the generalization to a multi dimensional parameter space where the deformation is induced by marginal operators spanning a moduli space (section 1.5).

1.1 Introduction to the Quantum Information Metric

A quantity that finds application in condensed matter physics and information theory is fidelity [14]. For two generic quantum states A and B described by density matrices ρ_A and ρ_B we define the fidelity $F(\rho_A, \rho_B)$ by the following formula:

$$F(\rho_A, \rho_B) = \mathrm{tr}\sqrt{{\rho_A}^{1/2}\rho_B{\rho_A}^{1/2}} \tag{1.1.1}$$

where the trace is taken over the Hilbert space of all quantum states of the system.

When the states A and B are pure fidelity reduces to the absolute value of the overlap, i.e. if $\rho_A = |\Psi_A\rangle \langle\Psi_A|$ and $\rho_B = |\Psi_B\rangle \langle\Psi_B|$ we have that

$$F(\Psi_A, \Psi_B) = |\langle\Psi_A|\Psi_B\rangle|. \tag{1.1.2}$$

We now consider a one parameter family of states, parametrized by λ, with corresponding density matrix ρ_λ and we define the QIM $G_{\lambda\lambda}$ by considering fidelity between two states relative to infinitesimally close parameters, say λ and $\lambda + \delta\lambda$, and expanding in $\delta\lambda$:

$$F(\rho_\lambda, \rho_{\lambda+\delta\lambda}) = 1 - G_{\lambda\lambda}\delta\lambda^2 + \mathcal{O}(\delta\lambda^3). \tag{1.1.3}$$

We can generalize this concept to a multi dimensional parameter space with $\lambda = \{\lambda^a\}$ and $a = 1, ..., N$. The natural generalization is:

$$F(\rho_\lambda, \rho_{\lambda+\delta\lambda}) = 1 - \sum_{a,b=1}^{N} G_{ab}\delta\lambda^a\delta\lambda^b + \mathcal{O}(\delta\lambda^3). \tag{1.1.4}$$

Notice that the presence of a term linear in $\delta\lambda$ vanishes by unitarity.

1.2 The QIM for the vacuum state of a CFT living on $\mathbb{R}^{d-1} \times \mathbb{R}$.

In this section we firstly review the computation of the QIM for a CFT in its ground state. We then explain how to compute the same quantity holographically using a perturbative approach.

1.2.1 CFT computation

Let us consider a d-dimensional CFT with Euclidean Lagrangian $\mathcal{L}_0$. We deform the theory by adding to $\mathcal{L}_0$ a term of the form $\delta\lambda\mathcal{O}(x)$, where $\mathcal{O}$ corresponds to a conformal primary operator of the original theory with conformal dimension Δ and $\delta\lambda$ is a coupling constant. In order to distinguish between quantities computed in the unperturbed theory and quantities in the deformed theory we use respectively the subscripts 0 and 1.

We are interested in computing the absolute value of the overlap between the ground states of the two theories $|\langle\Psi_1|\Psi_0\rangle|$ at second order in $\delta\lambda$. In order to do that we use a path integral formalism.

We start by considering the overlap between the ground state of the undeformed theory $|\Psi_0\rangle$ and a generic state $|\tilde{\varphi}\rangle$. In a path integral language the quantity $\langle\tilde{\varphi}|\Psi_0\rangle$ can be obtained by considering an Euclidean evolution from $\tau = -\infty$ to $\tau = 0$ where the state $|\tilde{\varphi}\rangle$ is inserted. In equation:

$$\langle\tilde{\varphi}|\Psi_0\rangle = \frac{1}{\sqrt{Z_0}} \int_{\varphi(\tau=0)=\tilde{\varphi}} \mathcal{D}\varphi \exp\left(-\int_{-\infty}^{0} d\tau \int d^{d-1}x \mathcal{L}_0\right), \tag{1.2.1}$$

where Z_0 is the partition function of the unperturbed theory:

$$Z_0 = \int \mathcal{D}\varphi \exp\left(-\int_{-\infty}^{\infty} d\tau \int d^{d-1}x \mathcal{L}_0\right). \tag{1.2.2}$$

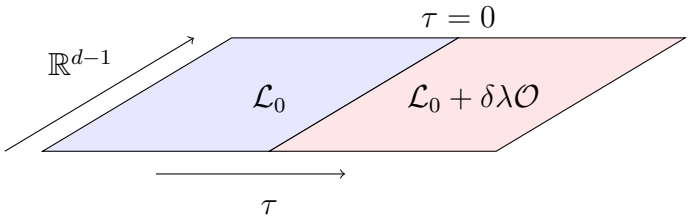

Figure 1.1: Pictorial representation of the path integral construction used to build $\langle\Psi_1|\Psi_0\rangle$. The Euclidean propagation is governed by the unperturbed Lagrangian $\mathcal{L}_0$ in the blue region, while in the red region we use the deformed Lagrangian $\mathcal{L}_0 + \delta\lambda\mathcal{O}$.

In a similar way we construct $\langle\Psi_1|\tilde{\varphi}\rangle$ by considering the Euclidean evolution from $\tau = 0$, where the state $|\tilde{\varphi}\rangle$ is inserted, to $\tau = \infty$:

$$\langle\Psi_1|\tilde{\varphi}\rangle = \frac{1}{\sqrt{Z_1}} \int_{\varphi(\tau=0)=\tilde{\varphi}} \mathcal{D}\varphi \exp\left(-\int_0^\infty d\tau \int d^{d-1}x(\mathcal{L}_0 + \delta\lambda\mathcal{O})\right), \tag{1.2.3}$$

with

$$Z_1 = \int \mathcal{D}\varphi \exp\left(-\int_{-\infty}^\infty d\tau \int d^{d-1}x(\mathcal{L}_0 + \delta\lambda\mathcal{O})\right) \tag{1.2.4}$$

being the partition function of the deformed theory. Notice that in this case we have used the deformed Lagrangian $\mathcal{L}_1 = \mathcal{L}_0 + \delta\lambda\mathcal{O}$.

The overlap $\langle\Psi_1|\Psi_0\rangle$ can then be obtained as

$$\begin{aligned} \langle\Psi_1|\Psi_0\rangle &= \int \mathcal{D}\tilde{\varphi}\, \langle\Psi_1|\tilde{\varphi}\rangle\, \langle\tilde{\varphi}|\Psi_0\rangle \\ &= \frac{\int \mathcal{D}\varphi \exp\left(-\int_{-\infty}^0 d\tau \int d^{d-1}x\mathcal{L}_0 - \int_0^\infty d\tau \int d^{d-1}x(\mathcal{L}_0 + \delta\lambda\mathcal{O})\right)}{(Z_0 Z_1)^{1/2}}. \end{aligned} \tag{1.2.5}$$

This overlap is generally speaking ill defined, since the Lagrangian governing the Euclidean propagation changes discontinuously at $\tau = 0$ and this introduces UV divergences. For this reason one should think of equation (1.2.5) as formal. For all explicit computations we regularize the UV divergences in the formula for the overlap (1.2.5) by replacing $|\Psi_1\rangle$ with

$$|\Psi_1(\epsilon)\rangle = \frac{e^{-\epsilon H_0}|\Psi_1\rangle}{\left(\langle\Psi_1|e^{-2\epsilon H_0}|\Psi_1\rangle\right)^{1/2}}, \tag{1.2.6}$$

where H_0 is the Euclidean Hamiltonian of the unperturbed theory. ϵ should be thought as an UV cut-off, its physical meaning might seem obscure at this point, but it will later become clear that ϵ removes the region where the Lagrangian changes abruptly .
We then rewrite equation (1.2.5) as an expectation value in the state $|\Psi_0\rangle$:

$$\langle\Psi_1(\epsilon)|\Psi_0\rangle = \frac{\langle\exp\left(-\int_\epsilon^\infty d\tau\int d^{d-1}x\delta\lambda\mathcal{O}(\tau,x)\right)\rangle}{\langle\exp\left(-(\int_{-\infty}^{-\epsilon}+\int_\epsilon^\infty)d\tau\int d^{d-1}x\delta\lambda\mathcal{O}(\tau,x)\right)\rangle^{1/2}}. \tag{1.2.7}$$

We can now expand the overlap (1.2.7) in powers of $\delta\lambda$. Taking into account that $\langle\mathcal{O}\rangle = 0$ for an operator of non-zero dimension in the unperturbed theory and that the two point function of a primary operator enjoys the time reversal symmetry relation $\langle\mathcal{O}(-\tau_1)\mathcal{O}(-\tau_2)\rangle = \langle\mathcal{O}(\tau_1)\mathcal{O}(\tau_2)\rangle$, we get that:

$$|\,\langle\Psi_1|\Psi_0\rangle\,| = 1 - G^\epsilon_{\lambda\lambda}\delta\lambda^2 + \mathcal{O}(\delta\lambda^3), \tag{1.2.8}$$

where

$$G^\epsilon_{\lambda\lambda} = \frac{1}{2}\int d^{d-1}x_1\int d^{d-1}x_2\int_{-\infty}^{-\epsilon}d\tau_1\int_\epsilon^\infty d\tau_2\,\langle\mathcal{O}(\tau_1,x_1)\mathcal{O}(\tau_2,x_2)\rangle \tag{1.2.9}$$

is the QIM. Notice that, as anticipated before, ϵ effectively removes a slab centered at $\tau = 0$.

The two point function for a primary operator is

$$\langle\mathcal{O}(\tau_1,x_1)\mathcal{O}(\tau_2,x_2)\rangle = \frac{\mathcal{N}_\Delta}{((\tau_1-\tau_2)^2+(x_1-x_2)^2)^\Delta} \tag{1.2.10}$$

with

$$\mathcal{N}_\Delta = \frac{\ell^{d-1}\,d\,\Gamma(\Delta)}{\kappa^2\pi^{\frac{d}{2}}\Gamma(\Delta-\frac{d}{2})} \tag{1.2.11}$$

where $\kappa^2 = 8\pi G$, with G being the $d+1$ dimensional Newton's constant and ℓ being the AdS radius scale appearing in the dual gravity description. This normalization is used to guarantee agreement between bulk and field theory side.

If $d+1-2\Delta<0$ we get:

$$G^{\epsilon}_{\lambda\lambda}=\mathcal{N}_{\Delta}N_{d}V_{\mathbb{R}^{d-1}}\epsilon^{d+1-2\Delta}, \tag{1.2.12}$$

where

$$N_{d}=\frac{2^{d-1-2\Delta}\pi^{(d-1)/2}\Gamma(\Delta-d/2-1/2)}{(2\Delta-d)\Gamma(\Delta)}. \tag{1.2.13}$$

Note that if we had to deform the theory by a linear combination of two primary operators, i.e. $\mathcal{L}_1=\mathcal{L}_0+\delta\lambda_A\mathcal{O}_A+\delta\lambda_B\mathcal{O}_B$, normalized such that $\langle\mathcal{O}_A\mathcal{O}_B\rangle=0$, the QIM would be diagonal. We will expand the discussion on multi dimensional parameter space in section 1.5 where we study the QIM in the case of a deformation induced by a linear combination of marginal operators spanning a moduli space.

1.2.2 Bulk computation

In this subsection we discuss the holographic dual of this setup. The computation of the QIM on the gravity side has appeared in [11] and [12] where $\mathcal{O}$ was taken to be exactly marginal. We develop a perturbative method that allows to deal with any primary (provided $\Delta>\frac{d+1}{2}$). The basic idea is to look at the right hand side of equation (1.2.5) and interpret is as a combination of partition functions. We have:

$$\langle\Psi_1|\Psi_0\rangle=\frac{Z_2}{(Z_1Z_0)^{1/2}}, \tag{1.2.14}$$

where Z_0 is the partition function of a pure CFT, Z_1 is the partition function of the deformed CFT and Z_2 is the partition function of a CFT that is deformed only for $\tau>0$.

We can evaluate these partition functions on the gravity side. In the large N limit we can write $Z_k=\exp(-I_k)$ where I_k is the on-shell action of the gravity solution dual to the corresponding field theory configuration ($k=0,1,2$). Since we consider the operator to have conformal dimension Δ the dual scalar field is going to have mass $m^2=\Delta(\Delta-d)$.

The action governing the bulk physics is

$$I = -\frac{1}{\kappa^2}\int d^{d+1}x\sqrt{g}\left(\frac{1}{2}R - \frac{1}{2}\partial_\mu\Phi\partial^\mu\Phi - \frac{1}{2}m^2\Phi^2 + \frac{d(d-1)}{2\ell^2}\right) + I_{BND}, \tag{1.2.15}$$

where the last term has been introduced in order to guarantee that the variational principle is well posed. The massive field is going to have a different profile in the three different cases of interest. In particular for the computation of Z_0 we notice that the massive field is turned off, the dual solution is pure AdS, then $Z_0 = \exp(-I_{\rm AdS})$.

The scalar field profile for I_1 and I_2 will depend on $\delta\lambda$. Since we are interested only in this quantities at order $\delta\lambda^2$ we can use a perturbative approach. We write the fields as[1]:

$$\Phi(x) = \delta\lambda\tilde{\Phi}(x), \tag{1.2.16}$$

$$g_{\mu\nu}(x) = g^0_{\mu\nu}(x) + \delta\lambda^2\tilde{g}_{\mu\nu}(x), \tag{1.2.17}$$

where $g^0_{\mu\nu}$ is the metric of pure AdS_{d+1}. Notice that the metric receives corrections at order $\delta\lambda^2$ since the scalar field enters quadratically in Einstein's equations.

We can now expand the on-shell action around the unperturbed solution

$$\begin{aligned}\delta I = {} & \delta\lambda\int\left.\frac{\delta I}{\delta\Phi(x)}\right|_{g_0}\tilde{\Phi}(x) + \frac{1}{2}\delta\lambda^2\int\left.\frac{\delta^2 I}{\delta\Phi(x)\delta\Phi(y)}\right|_{g_0}\tilde{\Phi}(x)\tilde{\Phi}(y) + \\ & + \delta\lambda^2\int\left.\frac{\delta I}{\delta g_{\mu\nu}(x)}\right|_{g_0}\tilde{g}_{\mu\nu}(x) + \mathcal{O}(\delta\lambda^3).\end{aligned} \tag{1.2.18}$$

Notice that the first and third terms vanish because the equations of motion of the background are satisfied. Notice also that the boundary term of equation (1.2.15) gets canceled by the boundary terms that arise from integration by parts when obtaining the first and third terms of equation (1.2.18). The second term of equation (1.2.18) should have been

[1]If the operator $\mathcal{O}$ is marginal the massless field should be taken to be $\Phi(x) = \lambda_0 + \delta\lambda\tilde{\Phi}(x)$, where λ_0 is the coupling constant of the undeformed theory.

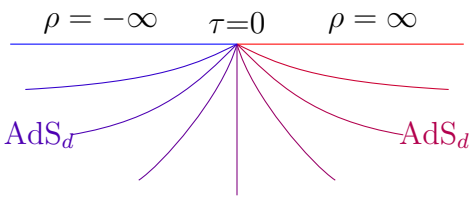

Figure 1.2: Schematic representation of the AdS$_d$ slicing of AdS$_{d+1}$. Each colored line corresponds to a single AdS$_d$ slice located at a fixed value of the coordinate ρ.

accompanied by the boundary term that arises when recasting the second variation of I in that guise. We omit it, since we will reintegrate the second term back by parts to bring δI in a form similar to the original one. It is now clear that we are simply interested in computing the contribution of the scalar field probing the unperturbed background. We can then write $I_k = I_{\rm AdS} + \delta I_k$, with

$$\delta I_k = \frac{1}{2\kappa^2}\int d^{d+1}x\sqrt{g_0}\left(g_0^{\mu\nu}\partial_\mu\Phi_k\partial_\nu\Phi_k + m^2\Phi_k^2\right). \tag{1.2.19}$$

Φ_k is the solution of the equation of motion of the massive field with fixed background. Φ_k can be obtained easily by using the boundary to bulk propagator:

$$\Phi_1(z,\tau,x) = z^{d-\Delta}\delta\lambda \tag{1.2.20}$$

$$\Phi_2(z,\tau,x) = \delta\lambda z^{d-\Delta}\left(\frac{\tau\Gamma\left(-\frac{d}{2}+\Delta+\frac{1}{2}\right)\,{}_2F_1\left(\frac{1}{2},-\frac{d}{2}+\Delta+\frac{1}{2};\frac{3}{2};-\frac{\tau^2}{z^2}\right)}{\sqrt{\pi}z\Gamma\left(\Delta-\frac{d}{2}\right)}+\frac{1}{2}\right) \tag{1.2.21}$$

We write the overlap as:

$$\begin{aligned}\langle\Psi_1|\Psi_0\rangle &= \frac{Z_2}{\sqrt{Z_1Z_0}} = \exp\left(-I_{\rm AdS}-\delta I_2+\frac{1}{2}(I_{\rm AdS}+\delta I_1+I_{\rm AdS})\right)\\ &= \exp\left(-\delta I_2+\frac{1}{2}\delta I_1\right).\end{aligned} \tag{1.2.22}$$

We now need to regularize the action δI_k $(k=1,2)$. We mentioned before that the back-

ground is Euclidean signature Poincaré AdS_{d+1}:

$$ds^2 = \ell^2 \frac{dz^2 + d\tau^2 + \sum_i^{d-1} dx_i^2}{z^2}, \tag{1.2.23}$$

the boundary is located at $z = 0$ and it is parametrized by (τ, x_i). We are going to work with AdS_{d+1} in AdS_d slicing by performing the following change of coordinates:

$$\begin{aligned} z &= Z \operatorname{sech} \rho \\ \tau &= Z \tanh \rho, \end{aligned} \tag{1.2.24}$$

the metric becomes

$$ds^2 = \cosh^2 \rho \left(\ell^2 \frac{dZ^2 + \sum_i^{d-1} dx_i^2}{Z^2} \right) + \ell^2 d\rho^2. \tag{1.2.25}$$

There are two different ways to reach the boundary: either we take $Z \to 0$ keeping ρ fixed or we take $\rho \to \pm\infty$ keeping Z fixed. In the first limit we reach the boundary at $(\tau = 0, x_i)$, while in second limit we reach the points $(\tau = \pm Z, x_i)$. The AdS_d slicing of AdS_{d+1} is schematically represented in figure 1.2.

We regularize the action by putting cut-offs at $\rho = \pm\rho_\infty$ and $Z = \epsilon$. We call the regularized manifold $\tilde{\mathcal{M}}$. This regularization choice might seem odd, since it is not the standard regularization condition used in many AdS/CFT examples. Chapter 2 is dedicated to discussing the validity of this regularization procedure, we refer to [3] for an exhaustive discussion of the subject. One could have adopted the usual regularization prescription by cutting off the AdS volume at $z = \delta$ obtaining the same results.

At this point one can easily work in the (ρ, Z, x_i) coordinates and evaluate δI_1 and δI_2. Assuming $2\Delta > d + 1$ we get the following result:

$$-\delta I_2 + \frac{1}{2}\delta I_1 = \frac{\mathrm{Vol}_{\mathbb{R}^{d-1}} \ell^{d-1} \epsilon^{d-2\Delta+1}}{2\kappa^2} (J_a + J_b + J_c)\delta\lambda^2 \tag{1.2.26}$$

where

$$J_a = \frac{1}{(2\Delta - d - 1)} \left((-f_2 \partial_\rho f_2 + f_1 \partial_\rho f_1) \cosh^d \rho \right) \Big|_{\rho_\infty}, \tag{1.2.27}$$

$$J_b = (d - \Delta) \int_0^{\rho_\infty} d\rho \left(-f_2^2(\rho) + f_1^2(\rho) \right) \cosh^{d-2} \rho \tag{1.2.28}$$

$$J_c = (d - \Delta) \int_{-\rho_\infty}^{0} d\rho \left(-f_2^2(\rho) \right) \cosh^{d-2} \rho. \tag{1.2.29}$$

The details of the computation can be found in [1]. Notice that J_a,J_b and J_c have no divergence associated with ρ_∞ and we are free to take the limit $\rho_\infty \to \infty$. J_a can be computed explicitly:

$$J_a = \frac{-d\Gamma\left(-\frac{d}{2} + \Delta + \frac{1}{2}\right)}{2(2\Delta - d - 1)\sqrt{\pi}\Gamma\left(-\frac{d}{2} + \Delta + 1\right)}. \tag{1.2.30}$$

The QIM is

$$G^{\epsilon}_{\lambda\lambda} = -\frac{\mathrm{Vol}_{\mathbb{R}^{d-1}} \ell^{d-1} \epsilon^{d-2\Delta+1}}{2\kappa^2} (J_a + J_b + J_c). \tag{1.2.31}$$

This matches the CFT result (1.2.12) in the sense that we recover the same divergence structure, we do not compare the coefficient of the divergence because it is a non universal quantity. Notice that, as in the CFT computation, the divergence arises only from the location where we turned on the deformation.

Note that if the operator $\mathcal{O}$ is marginal, i.e. $\Delta = d$, J_a and J_b vanish and we can write the result explicitly as:

$$G^{\epsilon}_{\lambda\lambda} = \frac{d\Gamma\left(\frac{d+1}{2}\right) \mathrm{Vol}_{\mathbb{R}^{d-1}} \ell^{d-1} \epsilon^{-d+1}}{4\sqrt{\pi}(d-1)\Gamma(\frac{d}{2}+1)\kappa^2}. \tag{1.2.32}$$

It is important to remark that the quantity computed is the bare QIM. Considering bare quantities and regularizing them by imposing a cut-off is usual practice in many AdS/CFT computations. The understanding is that, since the QIM is obtained by path integral arguments, one could make use of the standard holographic renormalization. The divergences can be removed by adding local counter terms to the bulk action. See [15] for a review on the topic. Finally, it is worth to point out that even the bare QIM has its own significance.

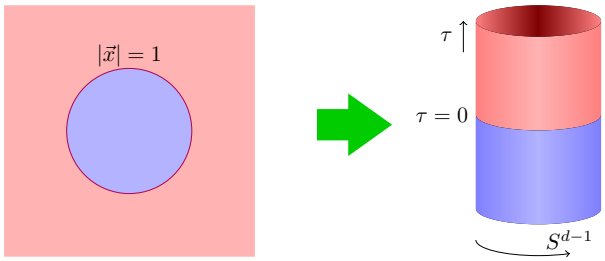

Figure 1.3: A map from $\mathbb{R}^d$ to $\mathbb{R} \times S^{d-1}$.

In fact it was the degree of the divergence of the bare QIM for a marginal deformation to suggest the brane approximation proposed in [11].

1.3 The QIM for the vacuum state of a CFT living on $\mathbf{S}^{d-1} \times \mathbb{R}$.

In this section we discuss the QIM obtained by studying deformation of the vacuum state of a CFT living on a cylinder. The CFT computation is analogous to the derivation showed in the section 1.2.1, the only difference being that the integration over the space slice is now performed on a sphere instead of a plane. For this reason we can write:

$$G^{\epsilon}_{\lambda\lambda} = \frac{1}{2} \int d^{d-1}\Omega_1 \sqrt{g_{\mathrm{S}^{d-1}}} \int d^{d-1}\Omega_2 \sqrt{g_{\mathrm{S}^{d-1}}} \int_{-\infty}^{-\epsilon} d\tau_1 \int_{\epsilon}^{\infty} d\tau_2 \, \langle \mathcal{O}(\tau_1, \Omega_1) \mathcal{O}(\tau_2, \Omega_2) \rangle \, . \quad (1.3.1)$$

For simplicity we have set the radius of the sphere r to one, i.e. we measure lengths in units of r. We eventually restore factors of r using dimensional analysis. The regularization procedure effectively removes a strip shaped region centered on $\tau = 0$. To compute $G^{\epsilon}_{\lambda\lambda}$ we need to use the two point function for a primary operator on the cylinder. We start with the two point function for $\mathbb{R}^d$ in Euclidean signature:

$$\langle \mathcal{O}(\tau_P, x) \mathcal{O}(\tau'_P, x') \rangle = \frac{\mathcal{N}_\Delta}{[\,(\tau_P - \tau'_P)^2 + (x - x')^2\,]^\Delta} \quad (1.3.2)$$

where τ_P indicates the Euclidean time on the plane.

Since the metric of Euclidean signature $\mathbb{R}^d$

$$ds^2 = d\tau_P^2 + \sum_i^{d-1} (dx^i)^2 = d\xi^2 + \xi^2 ds^2_{\mathrm{S}^{d-1}} \tag{1.3.3}$$

and the metric of the cylinder

$$ds^2 = d\tau^2 + ds^2_{\mathrm{S}^{d-1}} \tag{1.3.4}$$

are related by the conformal transformation $\xi = \exp(\tau)$, we can easily find the following expression for the two point function on the cylinder

$$\langle \mathcal{O}(\tau_1, \Omega_1)\mathcal{O}(\tau_1, \Omega_2\rangle = \frac{\mathcal{N}_\Delta}{(2\cosh(\tau_1 - \tau_2) - 2\Omega_1 \cdot \Omega_2)^\Delta}. \tag{1.3.5}$$

We depict the corresponding conformal map in Fig. 1.3. The form of the two point function implies that in the $\epsilon \to 0$ limit one gets the following leading behavior for the quantum information metric

$$G^\epsilon_{\lambda\lambda} \approx \epsilon^{d-2\Delta+1}. \tag{1.3.6}$$

This is not a surprise. In fact we recover the same leading behavior as the case of a CFT living in flat space [1, 11, 12].

What makes the configuration on the cylinder more interesting is the existence of a physical universal contribution. In addition, even if flat space and the cylinder are conformally equivalent, the quantum information metric on the cylinder cannot be inferred in general by the knowledge of the quantum information metric in flat space. This is due to the fact that we are turning on dimension-full coupling constants in the path integral formulation which results in the breaking of conformal symmetry.

Focusing on integer values of the conformal dimension Δ and taking $\Delta > (d+1)/2$ to avoid the issue of infrared divergences, one can show that the regularized QIM admits the

following expansion in ϵ [2]:

$$G^{\epsilon}_{\lambda\lambda} = a_{-2\Delta+d+1}\left(\frac{\epsilon}{r}\right)^{-2\Delta+d+1} + a_{-2\Delta+d-1}\left(\frac{\epsilon}{r}\right)^{-2\Delta+d-1} + \cdots + a_0 + b_0 \log\frac{\epsilon}{r} + \mathcal{O}(\epsilon) \quad (1.3.7)$$

where we have restored the radius r of the spatial sphere where the CFT lives. The logarithmic term is present only when d is odd.

To extract the universal piece one has in general to construct counterterms that need to be added to action. This is a standard procedure in QFT. We choose to work in the minimal subtraction scheme. Once the power divergences are removed we can identify the universal piece in

$$G_{\lambda\lambda} = \begin{cases} -b_0 \log \mu r & \text{if } d \text{ is odd} \\ a_0 & \text{otherwise.} \end{cases} \quad (1.3.8)$$

where μ is the renormalization scale. This is can be explained heuristically when $\Delta = d$. In fact the path integral formulation can be interpreted as the partition function of a field theory with a conformal defect. The conformal defect lives in $d-1$ dimension, it is not a surprise that the anomalous term (logarithmic divergence) appears for d odd.

The computation of $G_{\lambda\lambda}$ is in principle a well posed problem and it is easy to work on specific cases, however it seems that a generic derivation of $G_{\lambda\lambda}$ is difficult to obtain. Based on numerous checks performed on both the CFT and on the bulk side [2] we propose that the universal contribution of the quantum information metric for a CFT living on the cylinder deformed by a scalar primary operator is given by

- d even:

$$G_{\lambda\lambda} = \ell^{d-1}\frac{d}{8\kappa^2}(-1)^{[\Delta-\frac{d-1}{2}]}\frac{\left[\Gamma(\frac{\Delta}{2})\Gamma(\frac{\Delta}{2}-\frac{d-2}{2})\right]^2}{\Gamma(\Delta-\frac{d}{2})\Gamma(\Delta-\frac{d-2}{2})}\mathrm{Vol}_{S^{d-1}} \quad (1.3.9)$$

where $\text{Vol}_{\text{S}^{d-1}}$ is the volume of unit S^{d-1} given by

$$\text{Vol}_{\text{S}^{d-1}} = \frac{2\pi^{\frac{d}{2}}}{\Gamma(\frac{d}{2})} \tag{1.3.10}$$

- d odd:

$$\begin{aligned} G_{\lambda\lambda} &= G^{\log}_{\lambda\lambda} \log \mu r \\ G^{\log}_{\lambda\lambda} &= = \ell^{d-1} \frac{d}{8\kappa^2} (-1)^{[\Delta - \frac{d-1}{2}]} \frac{\left[\Gamma(\frac{\Delta}{2})\Gamma(\frac{\Delta}{2} - \frac{d-2}{2})\right]^2}{\Gamma(\Delta - \frac{d}{2})\Gamma(\Delta - \frac{d-2}{2})} \text{Vol}_{\text{S}^{d-1}} \left(-\frac{2}{\pi}\right). \end{aligned} \tag{1.3.11}$$

As a final remark we discuss the connection between our results and the brane model [11]. If the deformation is induced by a marginal operator, one can use the brane model to compute the QIM on the bulk. The brane model is defined up to an overall constant, n_d, the tension of the brane. This constant can be fixed by comparing the brane model with the result of this section. One finds:

$$n_d = \frac{\ell^{d-1}\Gamma\left(\frac{1+d}{2}\right)}{2\kappa^2\sqrt{\pi}\Gamma(d/2)}, \tag{1.3.12}$$

however it is unclear how universal this quantity is.

1.4 Information metric and interface free energy of conformal Janus on S^d

In this section we relate the QIM on the cylinder to the free energy of a conformal Janus configuration on the Euclidean sphere.

As usual we start with the expression of the overlap between the deformed ground state and the undeformed one:

$$\langle \Psi_1 | \Psi_0 \rangle = \frac{Z_2}{\sqrt{Z_1 Z_0}} \tag{1.4.1}$$

We can compute the Z_k holographically by $Z_k = \exp(-I_k)$ where I_k is the on shell action of

a Einstein-dilaton theory. If the deformation is marginal we have

$$Z_0 = Z_1 = \exp(-I_{\mathrm{AdS}}), \tag{1.4.2}$$

and thus

$$\langle \Psi_1 | \Psi_0 \rangle = \exp(-(I_2 - I_{\mathrm{AdS}})). \tag{1.4.3}$$

If we expand the left hand side for small $\delta\lambda$ we have

$$\langle \Psi_1 | \Psi_0 \rangle = 1 - G_{\lambda\lambda}\delta\lambda^2 + \mathcal{O}(\delta\lambda^3) \tag{1.4.4}$$

Thus

$$\log(\langle \Psi_1 | \Psi_0 \rangle) = -G_{\lambda\lambda}\delta\lambda^2 + \mathcal{O}(\delta\lambda^3) = -(I_2 - I_{\mathrm{AdS}}), \tag{1.4.5}$$

which results in

$$\Delta F = G_{\lambda\lambda}\delta\lambda^2 + \mathcal{O}(\delta\lambda^3). \tag{1.4.6}$$

Therefore the free energy of a Janus interface at second order in the Janus deformation parameter reproduces the QIM for a CFT ground state living on $\mathbb{R} \times \mathrm{S}^{d-1}$.

At this point we want to relate the computation of the QIM on $\mathbb{R} \times \mathrm{S}^{d-1}$ to the computation of the free energy on S^d. We can map the cylinder to the sphere. A way to do this is to take the cylinder with metric

$$ds^2_{cyl} = d\tau^2 + ds^2_{\mathrm{S}^{d-1}} \tag{1.4.7}$$

and conformally map it to a sphere with metric

$$ds^2_{\mathrm{S}^d} = d\theta^2 + \sin^2\theta ds^2_{\mathrm{S}^{d-1}} \tag{1.4.8}$$

by using the following change of coordinates

$$\tau = \log(\tan(\theta/2)). \tag{1.4.9}$$

We are allowed to perform the change of coordinates because the fields well behave at $\tau = \pm\infty$. We will return on this detail later. Under the map (1.4.9) the interface at $\tau = 0$ is mapped to the equator of the sphere, the $\tau > 0$ (< 0) region is mapped to the northern (southern) hemisphere and the cut off surfaces $\tau = \pm\epsilon$ are mapped to cut off surfaces located at constant $\theta = 2\arctan(e^{\pm\epsilon})$.

To find the QIM on the cylinder one has to compute

$$\int_{\tau_1>\epsilon}\int_{\tau_2<-\epsilon} \langle \mathcal{O}(\tau_1,\Omega_1)\mathcal{O}(\tau_2,\Omega_2)\rangle \,. \tag{1.4.10}$$

Under the conformal transformation (1.4.9) this maps to

$$\int_{\tilde{N}}\int_{\tilde{S}} \langle \mathcal{O}(\theta_1,\Omega_1)\mathcal{O}(\theta_2,\Omega_2)\rangle \,, \tag{1.4.11}$$

where $\tilde{N}$ ($\tilde{S}$) indicates the (regularized) northern (southern) hemisphere Using a path integral construction we could have derived this formula by looking at the second order contribution in $\delta\lambda$ of ΔF_{sphere}. This indeed shows that we can compute the QIM for a marginal deformation by looking at the leading order contribution of the interface free energy.

This result can be checked analytically in the bulk. The interface free energy for the conformal Janus on the Euclidean sphere S^d has been computed in [16] for $d = 2, 3$ and indeed the small $\delta\lambda$ behavior matches the computation of the QIM presented in this chapter.

One could wonder if the same procedure can be applied for the QIM of a CFT living on $\mathbb{R}\times\mathbb{R}^{d-1}$. In this case the interface is a codimension one plane. A conformal transformation between this configuration and a sphere with interface extended along the equator is available. Before performing the conformal map one has to compactify the space. This is not

possible in this set up. The reason is that the interface extends to infinity, thus the fields generally speaking would have a non trivial behavior at large distances. We cannot therefore make the manifold compact.

The argument explained in this section fails if the deformation is not marginal. For a non marginal deformation the conformal transformation will change the effective source. Therefore the usual configuration on the cylinder would be mapped to a configuration on the sphere with a coupling constant that depends on the polar angle.

We conclude the section with a comment about regularization. On the cylinder the regularization is performed by excluding from the path integral the region close to the interface: we put cut offs at $\tau = \pm\epsilon$. These cut off surfaces are mapped to $\theta = 2\arctan(e^{\pm\epsilon}) \approx \pi/2 \pm \epsilon$, which looks appealing since it is the natural cut off one would use. However it is important to stress that generically one should make use of the entire expression $\theta = 2\arctan(e^{\pm\epsilon})$ since the relation between the cut offs in the two geometries is non linear and thus truncating the relation for small ϵ could suppress some potential finite contributions.

1.5 The QIM for a multi dimensional parameter space

In this section we show how to generalize the method used so far to the case of a multi dimensional parameter space.

We consider a CFT on a plane that has N coupling constants λ^a that couple to marginal operators. We change each coupling constant by an infinitesimal amount $\delta\lambda^a$. We are interested in studying the QIM in this set-up. We consider the absolute value of the overlap and expand it in $\delta\lambda$:

$$|\langle\Psi_{\lambda+\delta\lambda}|\Psi_\lambda\rangle| = 1 + G_{ab}\delta\lambda^a\delta\lambda^b + ... \tag{1.5.1}$$

As usual we write this overlap as a path integral where the value of each coupling constant is changed at $\tau = 0$.

On the bulk side we then must have N massless fields with nontrivial profile, dual to the

operators $\mathcal{O}_a$. In this context it is quite natural to study systems in which the bulk physics is governed by

$$I = -\frac{1}{\kappa^2}\int d^{d+1}x\sqrt{g}\left(\frac{1}{2}R - \frac{1}{2}\mathcal{G}_{ab}(\Phi)\partial_\mu\Phi^a\partial^\mu\Phi^b + \frac{d(d-1)}{2\ell^2}\right), \tag{1.5.2}$$

the term in the action involving the scalars is a non linear sigma model which parameterize a moduli space with metric $\mathcal{G}_{ab}$.

The reason for this choice is that the constant values of Φ^a around which we are perturbing correspond to moduli, which need to be allowed to be arbitrary for marginal operators.

The equations of motion are

$$-2\partial^\mu\left(\sqrt{g}\mathcal{G}_{ab}(\Phi)\partial_\mu\Phi^a\right) + \sqrt{g}\tfrac{\partial\mathcal{G}_{ac}(\Phi)}{\partial\Phi^b}\partial_\mu\Phi^a\partial^\mu\Phi^c = 0 \tag{1.5.3}$$

$$R_{\mu\nu} = \mathcal{G}_{ab}(\Phi)\partial_\mu\Phi^a\partial_\nu\Phi^b - \tfrac{d}{\ell^2}. \tag{1.5.4}$$

We now consider a perturbative expansion for the fields Φ^a. It is clear that the second term in equation (1.5.3) is of order $\delta\lambda^a\delta\lambda^c$. This means that at first order in $\delta\lambda^a$ the scalars decouple from each other and they probe an unperturbed background. The derivation is then analogous to the one parameter case. The profiles for the scalars reduce to:

$$\Phi^a(\rho) = \lambda^a + \frac{\delta\lambda^a}{I_d}\int_{-\infty}^{\rho}\frac{1}{\cosh^d(r)}dr, \tag{1.5.5}$$

where ρ is the coordinate that foliate AdS_{d+1} in AdS_d slices, as in equation (1.2.25), and $I_d = \int_{-\infty}^{\infty}\frac{1}{\cosh^d(r)}dr = \frac{2\sqrt{\pi}\Gamma\left(\frac{d}{2}+1\right)}{d\Gamma(\frac{d+1}{2})}$. The QIM is found to be

$$G^\epsilon_{ab} = \frac{d\Gamma\left(\frac{d+1}{2}\right)V_{\mathbb{R}^{d-1}}\ell^{d-1}\epsilon^{-d+1}}{4\sqrt{\pi}(d-1)\Gamma(\frac{d}{2}+1)\kappa^2}\mathcal{G}_{ab}(\lambda). \tag{1.5.6}$$

We notice that the information metric inherits the same tensor structure and symmetry structure as the metric of the space where the scalars live.

Chapter 2

Regularization of Entanglement Entropy in Holographic Interface Theories

In the previous chapter we have seen explicit examples of how to compute the QIM, on both the CFT side and the bulk side. The QIM was suffering from UV divergences on the CFT side, the divergences were present also on the bulk side and they originated form the fact that AdS space has infinite volume.

This features is not special to the specific computations performed in Chapter 1, but it is a common characteristic of most AdS/CFT computations. Because of the ubiquity of divergences in extracting quantities in any AdS/CFT set up a systematic discussion is needed.

Usually the regularization scheme on the bulk side is based on the fact that an asymptotically AdS metric can be expressed in terms Fefferman-Graham coordinates [17]

$$ds^2 = \frac{dz^2}{z^2} + \frac{1}{z^2} g_{ij}(x,z) dx^i dx^j \tag{2.0.1}$$

where $g_{ij}(x, z)$ has a leading z independent term and terms falling off as $z \to 0$, whose exact form depend on the dimensionality and details of the theory.

The boundary of the asymptotic AdS metric is located at $z = 0$ and the theory is regulated by imposing a cut-off at $z = \delta$.

Unfortunately the construction of Fefferman-Graham coordinates which cover all of the boundary can be difficult, for example in systems with an interface (ICFT) or a defect (DCFT). In this chapter we discuss the regularization procedure for holographic interface or defect solutions which are commonly known as Janus solutions, where one solves the bulk gravitational equations for a metric which is warped with an AdS factor. For some other approaches to describe interface, defect or boundary CFTs holographically see e.g. [18–21].

In these cases the small z expansion used for the Fefferman-Graham construction turns out to be an expansion in small $z/x_\perp$, where $x_\perp$ denotes the field theory direction perpendicular to the defect. This dependence is dictated by scale invariance. The expansion breaks down close to the defect, where $x_\perp \to 0$. Thus there is a wedge bulk region originating from the defect that cannot be covered. In the case of a co-dimension one defect we have two different Fefferman-Graham coordinates patches that cover some portion of the bulk on the two sides of the defect and a region just behind the defect that cannot be covered. A schematic representation is given in figure 2.1.

This problem has been faced in literature in different ways. The authors of [22] connected

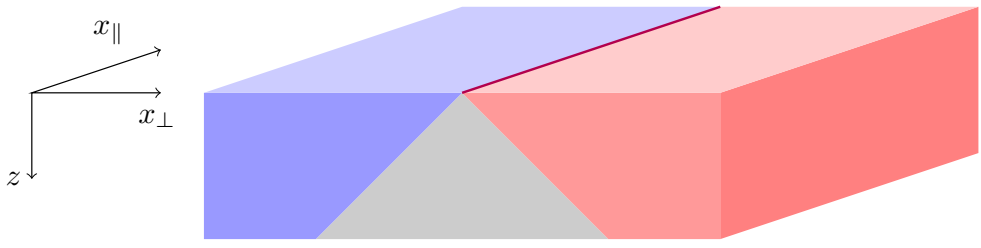

Figure 2.1: Fefferman-Graham coordinates for holographic ICFT. The top surface represents the field theory side, the two different colors identify the two sides of the interface (purple line). The vertical dimension represents the holographic direction, there are two Fefferman-Graham coordinate patches (represented with different colors) that do not cover the entire bulk geometry. In the gray wedge originating from the interface the Fefferman-Graham coordinate expansion breaks down.

the two Fefferman-Graham patches with an arbitrary curve, showing that any universal quantity would not depend on the details of this curve. To avoid dealing with Fefferman-Graham coordinates the authors of [16] simply imposed a cut off on the factor of the metric that diverges as one moves to the boundary. We refer to this regularization procedure as "single cut-off regularization".

As mentioned in Chapter 1 and as discussed in [1] a third regularization procedure has been used in literature in the computation of the QIM of a conformal theory which is deformed by a primary operator. Such a set up shares a lot of similarities with a DCFT [1,11,12] since it is natural to express the bulk metric using an AdS slicing. In such coordinates one encounters a divergence associated to the infinite volume of the AdS slice and a divergence associated to the coordinate that slices the bulk geometry. It is then natural to introduce two cut offs. We name this regularization procedure "double cut-off regularization". Note that an analogous cutoff was also used to regulate holographic duals of surface operators, i.e. defects of higher co-dimensionality in [23, 24].

In this chapter, based on [3], we study the double cut-off regularization procedure. This procedure has been tested against several examples to show that it provides the same results as the other regularization methods but involves much simpler computations.

2.1 Regularization prescriptions

To illustrate the different regularization procedures and their validity we mainly focus on the computation of entanglement entropy for a ball shaped region in a CFT with a co-dimension one interface. Notice however that the techniques that we will discuss can be used to the computation of any holographic quantity that requires regularization.

Entanglement entropy can be computed holographically as the area of the minimal bulk co-dimension two surface anchored at the boundary of AdS on the entangling surface [7]

$$S_{EE} = \frac{A_{\min}}{4G_N}. \tag{2.1.1}$$

this quantity is divergent because of the UV degrees of freedom entangled across the entangling surface. The regularization is achieved by introducing a UV cut-off. Once this is done if we want to isolate the interface contribution we need to subtract the entanglement entropy for the vacuum of the theory without interface. In this way we are able to compute a quantity that is intrinsic to the interface. To better explain this statement let us discuss in detail the divergence structure of entanglement entropy. For the vacuum state of a pure CFT and a ball shaped region of radius R we have:

$$S_{EE} = A_{d-2}\frac{R^{d-2}}{\delta^{d-2}} + ... + \begin{cases} A_1 \frac{R}{\delta} + s_0 & \text{if } d \text{ is odd} \\ A_2 \frac{R^2}{\delta^2} + s \log(2R/\delta) + \tilde{s}_0 & \text{if } d \text{ is even} \end{cases} \tag{2.1.2}$$

where we have introduced the UV cut-off δ [25]. Notice that in odd dimensions a rescaling of the cut-off does not affect constant s_0, while in even dimension it is the coefficient of the logarithmic term, s, that is not sensitive to any rescaling of δ. For this reason s and s_0 are independent of regularization and are universal. Let us discuss how the presence of a defect affects the structure of entanglement entropy. For definiteness we start with the vacuum state of an even dimensional CFT. We then turn on a co-dimension one interface that breaks the full conformal symmetry group $SO(2, d)$ down to $SO(2, d-1)$, interpreted as the conformal symmetry restricted to the interface. When this is done we expect the entanglement entropy to show terms typical of both even and odd dimensional CFTs [26]. That creates a problem in isolating the universal term characterizing the interface. In fact since the interface is odd dimensional we expect that the universal term should be a constant, however since the original CFT is even dimensional we have a logarithmic term in the divergence structure of the entanglement entropy and we are free to change the additive constant by a rescaling of the cut-off δ. The way to bypass this problem is to use the same cut-off for both the pure CFT and the ICFT, once that is done we can isolate the interface contribution by subtracting the vacuum component. We refer to this procedure as vacuum subtraction.

Now that we have discussed regularization and vacuum subtraction on the CFT side of the duality let's focus on the bulk side, where all the computations will be performed. First of all we need to identify a bulk geometry dual to the interface CFT. This is realized by a metric that is invariant under $SO(2, d-1)$ transformations. The natural way to do that is to consider a bulk geometry $\mathcal{M}$ that can be written in AdS_d slices:

$$ds^2 = A(x, y^a)^2 g_{\text{AdS}_d} + \rho(x, y^a)^2 dx^2 + G_{bc}(x, y^a) dy^b dy^c. \tag{2.1.3}$$

The coordinate x is taken to be non compact and as $x \to \pm\infty$ we have $A(x, y^a) \approx L_\pm \exp(\pm x + c_\pm)/2$ and $\rho(x, y^a) \approx 1$ such that the AdS_d gets enhanced to AdS_{d+1}. Unless otherwise stated we will work in Poincaré coordinates for the AdS_d slices

$$g_{\text{AdS}_d} = \frac{1}{Z^2}(Z^2 - dt^2 + dr^2 + r^2 g_{\text{S}^{d-3}}). \tag{2.1.4}$$

The boundary is approached in different ways. Taking $x \to \pm\infty$ we recover the CFT region on the right/left side of the interface, while taking $Z \to 0$ we approach the CFT on the interface itself.

We will now describe how to regularize divergent quantities on the bulk side using three different methods.

- **Fefferman-Graham regularization**: The traditional approach is to make use of Fefferman-Graham coordinates. As already mentioned this is problematic in a bulk

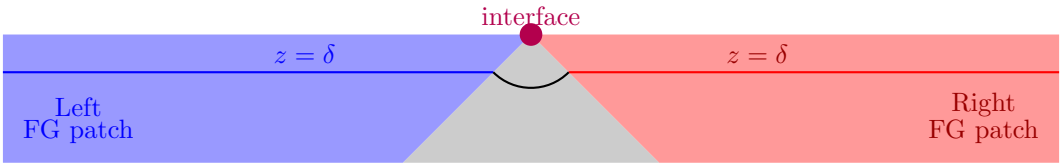

Figure 2.2: Schematic representation of the Fefferman-Graham regularization. Where the Fefferman-Graham coordinates are available (red and blue regions) the cut off surface is chosen to be $z = \epsilon$. In the middle region a Fefferman-Graham coordinate patch is not available. The cut off surface for this region is an arbitrary curve that continuously interpolates between the left and right patches, this is represented by a black arc in the picture.

geometry that is dual to a CFT with a defect or interface. There are two Fefferman-Graham patches which do not overlap, so one cannot simply glue them together. A possibility is then to interpolate with an arbitrary curve between these two patches, this is the approach used in [22] where the authors were able to compute universal quantities that do not depend on the interpolating curve. Even though this approach is very rigorous it requires a heavy computational effort. For this reason we want to explore other regularization procedures. A schematic representation of this procedure is given in figure 2.2.

- **single cut-off regularization**: we follow the idea of [16], regularizing all the divergent integrals by putting a cut-off at $Z/A(x) = \delta/L_{\pm}$. This is motivated by the study of pure AdS_{d+1}. In fact for pure AdS_{d+1} with unit radius one has $A(x) = \cosh x$, we can then change coordinates to recover Poincaré AdS_{d+1} by choosing:

$$z = \frac{Z}{\cosh x} \qquad \tilde{x} = Z \tanh x, \tag{2.1.5}$$

where z is the holographic coordinate and $\tilde{x}$ is the coordinate perpendicular to the fictitious interface. The natural cut-off procedure $z = \delta$ corresponds, in the AdS_d slicing coordinates, to $Z/A(x) = \delta$. For the interface solution which can be viewed as a deformation away from the AdS vacuum we keep the same regularization procedure.

- **double cut-off regularization**: this procedure is based on the observation that, after one performs the vacuum subtraction, one should be left with a quantity that is intrinsic to the interface. In that sense a cut-off should be imposed not on the full bulk geometry but on the AdS_d slices, at $Z = \delta$. Of course that cut-off does not regulate all the possible divergences, since the metric factor in (2.1.3) diverges as $A(x) \approx L_{\pm} \exp(\pm x + c_{\pm})/2$ as $x \to \pm\infty$. What one should do is to introduce a second cut-off ϵ, such that $A(x) = L_{\pm}\epsilon^{-1}$, that regulates any x dependent divergence. The presence of two cut offs might seem odd since on field theory side there should we a

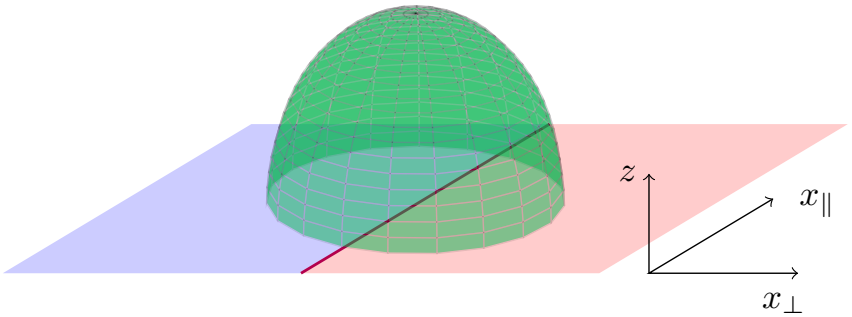

Figure 2.3: Ryu-Takayanagi surface. In this figure we represent a time slice of the field theory side. Two regions (blue and red) are separated by a interface (purple). We compute the holographic entanglement entropy for a ball centered on the interface. The Ryu-Takayanagi surface is represented in green.

single cut off that regulates all the the UV divergences. In the presence of the interface we can distinguish between degrees of freedom localized at or near the interface and degrees of freedom in the bulk away from the interface. Hence both cutoffs δ and ϵ have a physical interpretation.

In presence of Fefferman-Graham coordinates one should be able to relate δ to ϵ, we would then be left with a single regulator also on the bulk side. However, as mentioned above, the Fefferman-Graham coordinates do not cover the bulk geometry near the interface. We are able to bypass the problem in the following way: we leave the two cut offs δ and ϵ completely independent, any desired bulk quantities (such that entanglement entropy) can then be computed, since all divergent terms have been regulated by δ and ϵ. Once we subtract the vacuum contribution we will be allowed to take $\epsilon \to 0$, the result will be ϵ independent. The cutoff δ is interpreted as a physical cut-off in the usual sense, it regulates the bulk divergence associated to the AdS_d integration and it is interpreted as a UV cut-off for the degrees of freedom localized on the interface.

2.2 Explicit example: Regularization of Holographic Entanglement Entropy

This discussion applies to any divergent quantities that can be computed in a holographic ICFT. Let us now focus on the computation of holographic entanglement entropy. We take the entangling surface to be a ball shaped region of radius R centered on the interface (see figure 2.3). The holographic entanglement entropy for these systems has been studied in [26], where the authors were able to show that the RT surface is simply given by $r^2 + Z^2 = R^2$, giving the following expression for the entanglement entropy

$$S = \frac{\mathrm{Vol}_{\mathrm{S}^{d-3}}\, R}{4G_N} \int dy^a dx dZ \sqrt{\mathrm{det} G}\, \rho A^{d-2} \frac{(R^2 - Z^2)^{(d-4)/2}}{Z^{d-2}}. \tag{2.2.1}$$

This equation can be adapted also for $d = 3$ by taking $\mathrm{Vol}_{\mathrm{S}^0} = 2$.

Let us discuss how to regulate the entanglement entropy using the single and double cut-off regularizations. For the double cut-off procedure we cut-off the x integral at $x = x'_{\pm}$, defined as the two roots of $A(x') = L_{\pm}\epsilon^{-1}$. In most examples $A(x)^2$ is an even function, in that case $x'_+ = -x'_-$, we can then focus only on $x \in [0, x'_+]$ and we will drop the subscript. Generally speaking the form of A might be very complicated, however since ϵ eventually goes to zero we can assume x' large, allowing us to find $x'_{\pm} = \pm\left(\log(2/\epsilon) - c_{\pm}\right)$. We introduce a cut-off for the Z integration at $Z = \delta$. We then get:

$$\Delta S = \frac{\mathrm{Vol}_{\mathrm{S}^{d-3}}\, R}{4G_N} \left(\int_{\delta}^{R} dZ \frac{(R^2 - Z^2)^{(d-4)/2}}{Z^{d-2}} \right) \int dy^a \Delta \left(\int_{x_-}^{x_+} dx \sqrt{\mathrm{det} G}\, \rho A^{d-2} \right), \tag{2.2.2}$$

where the Δ symbol denotes the vacuum subtraction. At this point we will take $\delta, \epsilon \to 0$. The divergence will come exclusively from the Z integral and the result will be ϵ independent. This statement can be verified explicitly by similar arguments used in the appendix of [22].

In particular after the vacuum subtraction the divergence structure of the result is

$$\Delta S = C_{d-3}\frac{R^{d-3}}{\delta^{d-3}} + ... + \begin{cases} C_1 \frac{R}{\delta} + c_0 & \text{if } d \text{ is even} \\ C_2 \frac{R^2}{\delta^2} + c \log(2R/\delta) + \tilde{c}_0 & \text{if } d \text{ is odd,} \end{cases} \tag{2.2.3}$$

where all the dependence on the cutoff ϵ has disappeared. For all the examples we have studied the results we find agree with this general form. It would be interesting to show the agreement independently of any specific example.

We will now discuss the single cut-off procedure for the entanglement entropy. The general strategy is to put a cut-off at $Z/A(x) = \delta/L_{\pm}$. Then one proceeds by performing the x integral first and then the Z integral. To do so we start by fixing Z and integrating in x over $[\tilde{x}_-, \tilde{x}_+]$, where $\tilde{x}_{\pm}$ are the solutions to $Z/A(x) = \delta/L_{\pm}$. At this point we might be tempted to take δ small, however that is not possible. The reason for it is that the integration over Z runs over $[\min(A)\delta/L_{\pm}, R]$, where $\min(A)$ denotes the minimum of A (in most examples that corresponds to $x = 0$). Nonetheless we can expand $\exp(\tilde{x}_{\pm})$ as a Laurent series in δ/Z. Once this is done we will proceed to the integration, whose details depend on the concrete examples we will examine.

Notice that one could work in different coordinates than (2.1.3). In particular one could change coordinates from x to another coordinate, say q. The function $A(x)$ will then be replaced with another function, say $B(q)$. In that case the regularization procedures just described will go through without any change, one would simply put a cut-off for the q integration at $B(q) = L_{\pm}\epsilon^{-1}$ for the double cut-off procedure and at $B(q) = L_{\pm}Z\delta^{-1}$ for the single cut-off procedure.

Using these regularization procedures we computed ΔS holographically for the interface conformal field theories dual to the following bulk configurations:

- **Supersymmetric Janus**. The Supersymmetric Janus is the bulk dual for a Yang-Mills interface that preserves 16 supercharges [27, 28]. That is realized in the bulk

by a metric that exhibits $SO(2,3) \times SO(3) \times SO(3)$ symmetry, where the first factor is associated to the conformal symmetry of the interface and the other two factors are related to the unbroken R-symmetry. The full supergravity solution has also the dilaton, the three-form and the five-form turned on in the bulk.

- **Non Supersymmetric Janus**. The non Supersymmetric Janus is a solution of type IIB supergravity that can be thought as a deformation of the vacuum solution $\mathrm{AdS}_5 \times \mathrm{S}^5$ [13, 29]. The deformation depends on a real parameter $\gamma \in [3/4, 1]$, where $\gamma = 1$ corresponds to the vacuum solution. The metric is supported by a non trivial dilaton and RR five-form. This solution breaks all supersymmetries. The bulk configuration is interpreted as being dual to a deformation of $\mathcal{N} = 4$ SYM, where an interface is present and the Yang Mills coupling constant takes different values on the two sides of the interface.

- **Einstein-Dilaton Janus**. We can engineer a ICFT from a CFT by considering a marginal operator $\mathcal{O}$ and assigning it a coupling constant that jumps across the interface. We can construct the bulk theory dual to this deformation by solving the equations of motion derived from the action of a massless field dual to $\mathcal{O}$ minimally coupled to the metric [12]. The solution depends on a parameter $\lambda \in [0, \sqrt{d-1}\left(\frac{d-1}{d}\right)^{\frac{d-1}{2}}]$ that quantifies the strength of the deformation. The case $\lambda = 0$ corresponds to the undeformed solution.

- **M-theory Janus**. The M-theory Janus solution is a one parameter deformation of the $\mathrm{AdS}_4 \times \mathrm{S}^7$ vacuum solution of the eleven dimensional supergravity [30]. The dual field theory is ABJM theory deformed by a primary operator of dimension two localized on a interface.

The details of the computation can be found in [3]. We find that the universal piece of ΔS does not depend on the chosen regularization procedure and agrees with the result obtained using the Fefferman-Graham regularization [22].

2.3 Two dimensional holographic interfaces

It has been observed in various contexts that in a three dimensional CFT with a two dimensional conformal defect one can associate an effective central charge to the defect [24,31,32]. This central charge appears both in the entanglement entropy and in the Weyl-anomaly of the theory.

The fact that we can identify an effective central charge can be understood holographically. The argument is that when a 1+1 dimensional interface enjoys conformal symmetry we expect the dual bulk geometry to present an AdS_3 factor, we can thus associate an effective central charge to the interface through the Brown-Henneaux formula [33]. This was first done in [24] in the context of type IIB supergravity solutions dual to half-BPS disorder-type surface defects in $\mathcal{N} = 4$ Super Yang-Mills theory. It was also observed that the effective central charge arising from the Brown-Henneaux formula was the same quantity that appears in the computation of the entanglement entropy.

The M-theory Janus and the d=3 Einstan-Dilaton Janus are examples in which the 1+1 interface is embedded in a 3 dimensional theory. In addition to the computation of entanglement entropy one can calculate the conformal anomaly and show that it is governed by the same central charge appearing in the entanglement entropy computation and arising from the Brown-Henneaux formula.

The discussion of the explicit examples can be found in [3], here we prove the following statement:

In an ICFT with an even dimensional interface embedded into an odd dimensional spacetime the universal contribution of entanglement entropy for a spherical entangling surface centered on the interface is equal to minus the universal term of the free energy on a sphere.

We explicitly prove this statement for a 3 dimensional theory with a 2 dimensional interface. The generalization to arbitrary dimensions is straightforward. The proof follows

closely section 4 of [34]. The field theory lives on a three dimensional spacetime given by:

$$ds^2 = -dt^2 + d\rho^2 + \rho^2 d\phi^2, \tag{2.3.1}$$

where we have chosen polar coordinate for the spatial slice. The interface is located at $\sin\phi = 0$. We perform the following change of coordinates:

$$\begin{aligned} t &= \frac{R\cos\eta\sinh(\tau/R)}{1+\cos\eta\cosh(\tau/R)} \\ \rho &= R\frac{\sin\eta}{1+\cos\eta\cosh(\tau/R)}. \end{aligned} \tag{2.3.2}$$

The spacetime is then given by

$$\begin{aligned} ds^2 &= \Omega^2(-\cos^2\eta d\tau^2 + R^2(d\eta^2 + \sin^2\eta d\phi^2)) \\ \Omega &= (1+\cos^2\eta\cosh(\tau/R))^{-1}, \end{aligned} \tag{2.3.3}$$

which, after removing Ω, corresponds to the static patch of de Sitter space with curvature scale R. It can be shown (for details see [34]) that the new coordinates cover the causal development of the ball $\rho < R$ on the surface $t = 0$ (which is exactly our entangling region). In addition one can show that the modular flow generated by the modular Hamiltonian in the causal diamond corresponds to time flow in this new coordinate system and that original density matrix can be written as a thermal density matrix with temperature $T = 1/(2\pi R)$. This implies that the entanglement entropy of the ball shaped region can be written as a thermal entropy:

$$S = \beta E - W, \tag{2.3.4}$$

where W is the free energy and E is the expectation value of the operator which generates

time evolution, explicitly:

$$E = \int_V d^2x\sqrt{h}\,\langle T_{\mu\nu}\rangle\,\xi^\mu n^\nu = -\int_V d^2x\sqrt{-g}\,\langle T^\tau{}_\tau\rangle\,, \tag{2.3.5}$$

where V is a constant τ slice, n is the unit normal $n^\mu\partial_\mu = \sqrt{|g_{\tau\tau}|}\partial_\tau$ and ξ is the Killing vector that generates τ translations $\xi^\mu\partial_\mu = \partial_\tau$.

To compute E we need to write an expression for $\langle T^\tau{}_\tau\rangle$. A powerful tool to do that is symmetry. In fact we know that the interface is extended along the surface $\sin\phi = 0$ which corresponds to a two dimensional de Sitter spacetime. The isometry of de Sitter space forces the stress tensor to satisfy the following relations:

$$\begin{aligned} \langle T^\alpha{}_\beta\rangle &= \tilde{c}\,\delta^\alpha{}_\beta\,\delta(\sin\phi) \\ \langle T^\phi{}_\beta\rangle &= \langle T^\alpha{}_\phi\rangle = \langle T^\phi{}_\phi\rangle = 0, \end{aligned} \tag{2.3.6}$$

where α and β denote any of the coordinates η and τ. This suffices to show that E is finite. On the other side, since the interface is even dimensional we expect a logarithmic divergence in both S and W. This means that E does not contribute to the universal terms in equation (2.3.4), thus:

$$S_{\text{UNIV}} = -W_{\text{UNIV}}. \tag{2.3.7}$$

In order to find W_{UNIV} we go to imaginary time with periodicity $2\pi R$. The metric becomes

$$ds^2 = \cos^2\theta d\tau^2 + R^2(d\theta^2 + \sin^2\theta d\phi^2), \tag{2.3.8}$$

which we recognize as the metric of S^3 once we identify $\tau \sim \tau + 2\pi R$. Thus:

$$S_{\text{UNIV}} = -W_{\text{UNIV}}(\mathrm{S}^3), \tag{2.3.9}$$

as anticipated.

We would like to relate this quantity to an effective central charge (since we are in presence of a two dimensional conformal field theory living on the interface). To do that we focus on $W_{\rm UNIV}(\mathrm{S}^3)$. For definiteness let's say we locate the interface at the equator of the sphere. By the same symmetry arguments as in the de Sitter case we have:

$$\begin{aligned} \langle T_{\vartheta\vartheta}\rangle &= \langle T_{\vartheta\alpha}\rangle = 0 \\ \langle T_{\alpha\beta}\rangle &= \frac{c_{\rm eff}}{24\pi r^2} h_{\alpha\beta}\delta\left(\vartheta - \frac{\pi}{2}\right), \end{aligned} \tag{2.3.10}$$

where α and β denotes the directions along the interface and h is the metric of the sphere

$$ds^2_{\mathrm{S}^3} = r^2\left(d\vartheta + \sin^2\vartheta ds^2_{\mathrm{S}^2}\right), \tag{2.3.11}$$

with $\vartheta \in [0,\pi]$ and $\vartheta = \pi/2$ corresponding to the location of the interface. If we change the radius of the sphere by δr we have:

$$\delta_r W_{\rm UNIV} = \frac{1}{2}\int_{\mathrm{S}^3} d^3x\sqrt{h}\delta h^{ij}\,\langle T_{ij}\rangle = -\frac{c_{\rm eff}}{3r}\delta r = -\frac{c_{\rm eff}}{3}\delta_r \log r, \tag{2.3.12}$$

where we have used equations (2.3.10) to get the final result. This shows that the coefficient of the logarithmic term of entanglement entropy is related to the coefficient of the Ricci scalar in the conformal anomaly[1].

Notice that a priori this is a non trivial fact. In a two dimensional CFT the only central charge is the coefficient of the Ricci scalar in the trace anomaly, but in a ICFT the situation is more complicated. In fact the 1+1 dimensional interface is embedded in a higher dimensional spacetime where the theory lives, thus other terms, such as the trace of the extrinsic curvature, could contribute to the trace anomaly.

[1]If the interface is even dimensional embedded into a odd dimensional spacetime of general dimension we have that the coefficient of the logarithmic term is related to the A anomaly.

Chapter 3

Investigating Type IIB Supergravity duals for 5d SCFTs via Holographic Entaglment Entropy and Free Energy

While the first two chapter are devoted to give a prescription to compute quantum information quantities holographically, in Chapters 3 and 4 we look at a concrete realization of AdS/CFT duality and explore features of the field theory though its holographic dual.

We restrict our focus to five dimensional super superconformal field theories (SCFTs). These theories are interesting for a variety of reasons. Their existence is not obvious, since Yang-Mills theories in 5d have a dimensionful coupling constant and are non-renormalizable by power counting. Therefore they can not be treated consistently in perturbation theory. Nevertheless, the classification of [35] states that there is a unique superconformal algebra with 16 supercharges in five dimensions, given by the superalgebra $F(4)$ [36]. Field theory analysis of the dynamics on the Coulomb branch indeed indicates that for large classes of combinations of gauge group and matter content, 5d super Yang-Mills theories admit a well-defined UV limit where the coupling constant diverges [37, 38].

There is no known standard Lagrangian description for the 5d SCFTs obtained as UV

fixed points of the gauge theories. However, the theories can be engineered using brane constructions in type IIA and IIB string theory [39–41], which further supports their existence and has led to many insights. In the absence of a conventional Lagrangian description, AdS/CFT dualities are a perfect tool for comprehensive quantitative analysis. Supergravity duals in type IIA supergravity have indeed been known for some time, but they are singular [42, 43]. Although the singular nature limits the kind of questions that can be addressed, remarkable checks have been carried out with these solutions. In [44] the free energy on S^5 was compared to a localization calculation in the putative dual field theory. Due to the singularities in the solutions, the holographic computation of the free energy had to proceed through the entanglement entropy of a spherical region, which is less sensitive to the singularities in the geometry.[1] But once obtained, it matched the localization calculation, lending strong support to the proposed holographic dualities.

More recently, large classes of holographic duals for 5d SCFTs have been constructed in type IIB supergravity [48–50], where the geometry takes the form of $AdS_6 \times S^2$ warped over a two-dimensional Riemann surface Σ.[2] The solutions are singular as well, and avoid a recent no-go theorem [56]. But in contrast to the type IIA solutions, the singularities are at isolated points which have a clear interpretation as remnants of the external 5-branes appearing in the brane-web constructions. Nevertheless, it is an interesting question whether or to what extent these singularities affect AdS/CFT computations.

This chapter is based on the results of [4], where the finite part of the entanglement entropy for a spherical region and the free energy of the field theory on S^5 were computed. The singularities present in the solution are mild enough to not interfere with the computation of either the free energy or the entanglement entropy. In fact, it appears that the poles also do not contribute a finite part in either calculation, which would be well in line with the interpretation that modes on the external 5-branes in brane web constructions decouple.

[1] Another strategy is to work in 6d gauged supergravity, where the singularities resulting from the brane construction in type IIA string theory are not visible [45–47].

[2] For earlier work on AdS_6 type IIB solutions see [51–55].

Moreover, the relation of the finite part of the entanglement entropy for a spherical region to the free energy on S^5 holds as expected on general grounds [34]. For the non-trivial geometries we are considering the equivalence depends on rather non-trivial identities and hence provides a strong consistency check.

3.1 Review of type IIB supergravity solutions

The type IIB supergravity solutions we consider in this chapter have been derived and discussed in detail in [48–50], and we will only give a brief review introducing the quantities that will be relevant for the computation of free energy and entanglement entropy.

The relevant bosonic fields of type IIB supergravity are the metric, the complex axion-dilaton scalar B and the complex 2-form $C_{(2)}$ [57,58]. The real 4-form $C_{(4)}$ and the fermionic fields vanish. The geometry of the solutions is $AdS_6 \times S^2$ warped over a Riemann surface Σ, which for the solutions considered here will be the upper half plane. With a complex coordinate w on Σ, the metric and the 2-form field are parametrized by scalar functions f_2^2, f_6^2, ρ^2 and $\mathcal{C}$ on Σ,

$$ds^2 = f_6^2\, ds^2_{AdS_6} + f_2^2\, ds^2_{S^2} + 4\rho^2 dw d\bar{w} \ , \qquad C_{(2)} = \mathcal{C}\, \mathrm{vol}_{S^2} \ . \tag{3.1.1}$$

The solutions are expressed in terms of two holomorphic functions $\mathcal{A}_\pm$ on Σ, which are given by

$$\mathcal{A}_\pm(w) = \mathcal{A}^0_\pm + \sum_{\ell=1}^{L} Z^\ell_\pm \ln(w - p_\ell) \ . \tag{3.1.2}$$

The p_ℓ are restricted to be on the real line and are poles with residues $Z^\ell_\pm$ in $\partial_w \mathcal{A}_\pm$. The residues are related by complex conjugation $Z^\ell_\pm = -\overline{Z^\ell_\mp}$. The explicit form of the solutions

is conveniently expressed in terms of the composite quantities

$$\kappa^2 = -|\partial_w \mathcal{A}_+|^2 + |\partial_w \mathcal{A}_-|^2 \ , \qquad \partial_w \mathcal{B} = \mathcal{A}_+ \partial_w \mathcal{A}_- - \mathcal{A}_- \partial_w \mathcal{A}_+ \ , \tag{3.1.3}$$

$$\mathcal{G} = |\mathcal{A}_+|^2 - |\mathcal{A}_-|^2 + \mathcal{B} + \bar{\mathcal{B}} \ , \qquad R + \frac{1}{R} = 2 + 6\,\frac{\kappa^2\,\mathcal{G}}{|\partial_w \mathcal{G}|^2} \ . \tag{3.1.4}$$

Regularity of the solutions requires that κ^2 and $\mathcal{G}$ are both positive in the interior of Σ and vanish on the boundary. These regularity conditions are satisfied if the residues are given by

$$Z_+^\ell = \sigma \prod_{n=1}^{L-2} (p_\ell - s_n) \prod_{k \neq \ell}^{L} \frac{1}{p_\ell - p_k} \ . \tag{3.1.5}$$

and the s_n are restricted to be in the upper half plane. Moreover, the p_ℓ and s_n have to be chosen such that they satisfy

$$\mathcal{A}^0 Z_-^k + \bar{\mathcal{A}}^0 Z_+^k + \sum_{\ell \neq k} Z^{[\ell k]} \ln |p_\ell - p_k| = 0 \ , \tag{3.1.6}$$

where $Z^{[\ell k]} \equiv Z_+^\ell Z_-^k - Z_+^k Z_-^\ell$ and $2\mathcal{A}^0 \equiv \mathcal{A}_+^0 - \bar{\mathcal{A}}_-^0$. The explicit form of the functions parametrizing the metric is then given by

$$f_6^2 = \sqrt{6\mathcal{G}} \left(\frac{1+R}{1-R}\right)^{1/2} \ , \quad f_2^2 = \frac{1}{9}\sqrt{6\mathcal{G}} \left(\frac{1-R}{1+R}\right)^{3/2} \ , \quad \rho^2 = \frac{\kappa^2}{\sqrt{6\mathcal{G}}} \left(\frac{1+R}{1-R}\right)^{1/2} \ , \tag{3.1.7}$$

where we used the expressions of [50] with $c_6^2 = 1$, which was shown there to be required for regularity. The function $\mathcal{C}$ parametrizing the 2-form field is given by

$$\mathcal{C} = \frac{4i}{9} \left(\frac{\partial_{\bar{w}} \bar{\mathcal{A}}_- \, \partial_w \mathcal{G}}{\kappa^2} - 2R\, \frac{\partial_w \mathcal{G}\, \partial_{\bar{w}} \bar{\mathcal{A}}_- + \partial_{\bar{w}} \mathcal{G}\, \partial_w \mathcal{A}_+}{(R+1)^2\, \kappa^2} - \bar{\mathcal{A}}_- - 2\mathcal{A}_+ \right) \tag{3.1.8}$$

and the axion-dilaton scalar B is given by

$$B = \frac{\partial_w \mathcal{A}_+\, \partial_{\bar{w}} \mathcal{G} - R\, \partial_{\bar{w}} \bar{\mathcal{A}}_- \partial_w \mathcal{G}}{R\, \partial_{\bar{w}} \bar{\mathcal{A}}_+ \partial_w \mathcal{G} - \partial_w \mathcal{A}_- \partial_{\bar{w}} \mathcal{G}} \ . \tag{3.1.9}$$

The crucial feature for the identification of the solutions with 5-brane webs is that the $2L-2$ free parameters of a solution with L poles can be taken as the residues Z_+^ℓ, subject to the constraint that $\sum_\ell Z_+^\ell = 0$. Combined with the observation that at each pole p_m the solution turns into a $(q_1, q_2)Q$ 5-brane solution, in the conventions of [59], with

$$(q_1 - iq_2)Q = \frac{8}{3} Z_+^m \ , \tag{3.1.10}$$

this gives a direct identification of the supergravity solutions with 5-brane intersections.

3.1.1 Killing spinors

These configurations solve the BPS equations for preserving sixteen supersymmetries, and as shown in [60] also the equations of motion. For later convenience we review also the form of the Killing spinors. We will use the Clifford algebra conventions summarized in appendix A of [48]. The ten-dimensional Killing spinor ϵ is expanded in terms of $\mathrm{AdS}_6 \times \mathrm{S}^2$ Killing spinors $\chi^{\eta_1\eta_2}$ and complex two-component spinors on Σ, $\zeta_{\eta_1\eta_2}$, as follows

$$\epsilon = \sum_{\eta_1,\eta_2=\pm} \chi^{\eta_1\eta_2} \otimes \zeta_{\eta_1\eta_2} \ , \tag{3.1.11}$$

and analogously[3] $C^{-1}\epsilon^\star = \sum_{\eta_1\eta_2} \chi^{\eta_1\eta_2} \otimes \star\zeta_{\eta_1\eta_2}$, with $\star\zeta_{\eta_1\eta_2} = -i\eta_2\sigma^2\zeta^\star_{\eta_1\,-\eta_2}$. In a chirality basis where σ^3 is diagonal, we have

$$\zeta_{++} = \begin{pmatrix} \bar\alpha \\ \beta \end{pmatrix} \ , \qquad \zeta_{--} = \begin{pmatrix} -\bar\alpha \\ \beta \end{pmatrix} \ , \qquad \zeta_{+-} = i\nu\zeta_{++} \ , \qquad \zeta_{-+} = i\nu\zeta_{--} \ . \tag{3.1.12}$$

[3]To avoid confusion with the composite quantity $\mathcal{B}$ defined in (3.1.3), we will denote the charge conjugation matrix by C throughout.

where $\nu \in \{-1, +1\}$ and, with $f^{-2} = 1 - |B|^2$,

$$\rho\bar{\alpha}^2 = f(\partial_w \mathcal{A}_+ + B\partial_w \mathcal{A}_-) \ , \qquad \rho\beta^2 = f(B\partial_{\bar{w}} \bar{\mathcal{A}}_+ + \partial_{\bar{w}} \bar{\mathcal{A}}_-) \ . \tag{3.1.13}$$

The action of the Clifford algebra elements on the Killing spinors that will be relevant in Chapter 4 are derived from the relation

$$(\gamma_{(1)} \otimes I_2)\chi^{\eta_1\eta_2} = \chi^{-\eta_1\eta_2} \ , \qquad (I_8 \otimes \gamma_{(2)})\chi^{\eta_1\eta_2} = \chi^{\eta_1\,-\eta_2} \ , \tag{3.1.14}$$

where $\gamma_{(i)}$ denotes the chirality matrices on the respective components of $\mathrm{AdS}_6 \times \mathrm{S}^2 \times \Sigma$ (see appendix A of [48] for more details). From these one concludes that

$$\begin{aligned} \Gamma^{01234567}\epsilon &= -i \sum_{\eta_1\eta_2} \chi^{\eta_1\eta_2} \otimes \zeta_{-\eta_1\,-\eta_2} \ , \\ \Gamma^{67}\Gamma^{01234567}C^{-1}\epsilon^\star &= \sum_{\eta_1\eta_2} \chi^{\eta_1\eta_2} \otimes \star\zeta_{-\eta_1\eta_2} \ . \end{aligned} \tag{3.1.15}$$

3.2 On-shell action and free energy on S^5

In this section we review the computation of the on-shell action for the solutions presented in the previous section. Formulating an action for type IIB supergravity is subtle due to the self-duality constraint on the 4-form potential, but since $C_{(4)} = 0$ in our solutions this is not an issue. Moreover, the on-shell action can be expressed as a boundary term [61]. We have:

$$\begin{aligned} S^{\mathrm{E}}_{\mathrm{IIB}} &= \frac{1}{64\pi G_{\mathrm{N}}} \int_{\mathcal{M}} d\left[\frac{1}{2} f^2 (1 + |B|^2)\, \bar{C}_2 \wedge \star dC_2 - f^2 \bar{B} C_2 \wedge \star dC_2 + \text{c.c.}\right] \\ &= \frac{1}{64\pi G_{\mathrm{N}}} \int_{\partial\mathcal{M}} f^2 \left[\frac{1}{2}(1 + |B|^2)\bar{C}_2 - \bar{B} C_2\right] \wedge \star dC_2 + \text{c.c.} \end{aligned} \tag{3.2.1}$$

where $f^{-2} = 1 - |B|^2$. We now use that $C_2 = \mathcal{C}\text{vol}_{\text{S}^2}$, where vol_{S^2} is the volume form on the S^2 of unit radius. This yields

$$\star dC_2 = f_6^6 f_2^{-2} \text{vol}_{\text{AdS}_6} \wedge \star_\Sigma d\mathcal{C} \ , \tag{3.2.2}$$

where $\text{vol}_{\text{AdS}_6}$ is the volume form on AdS_6 of unit curvature radius and $\star_\Sigma$ is the Hodge dual on Σ with metric $g_\Sigma = 4\rho^2 |dw|^2$. We then find

$$S_{\text{IIB}}^{\text{E}} = \frac{1}{64\pi G_{\text{N}}} \int_{\partial M} f^2 f_6^6 f_2^{-2} \left[\frac{1}{2}(1 + |B|^2)\bar{\mathcal{C}} - \bar{B}\mathcal{C} \right] \text{vol}_{\text{S}^2} \wedge \text{vol}_{\text{AdS}_6} \wedge \star_\Sigma d\mathcal{C} + \text{c.c.} \tag{3.2.3}$$

The AdS_6 volume can be regularized and renormalized in the usual way for an AdS_6 with unit radius of curvature and we will just use $\text{Vol}_{\text{AdS}_6,\text{ren}}$ to denote the renormalized volume. One can show that there are no finite contributions to the on-shell action from the boundary introduced when regularizing the AdS_6 volume. The explicit expression for the renormalized volume of global AdS_6 with a renormalization scheme preserving the S^5 isometries of the sphere is

$$\text{Vol}_{\text{AdS}_6,\text{ren}} = -\frac{8}{15} \text{Vol}_{\text{S}^5} \ , \tag{3.2.4}$$

for details see the appendix of [4]. Note that we denote by e.g. Vol_{S^5} the actual volume, i.e. $\text{Vol}_{\text{S}^5} = \int_{\text{S}^5} \text{vol}_{\text{S}^5}$. The only (remaining) boundary then is the boundary of Σ. We note that $\partial\Sigma$ is not an actual boundary of the ten-dimensional geometry, so in particular there are no extra boundary terms to be added, but for the evaluation of the on-shell action as a total derivative we have to take it into account. We thus find

$$S_{\text{IIB}}^{\text{E}} = \frac{1}{64\pi G_{\text{N}}} \text{Vol}_{\text{AdS}_6,\text{ren}} \text{Vol}_{\text{S}^2} \int_{\partial\Sigma} f^2 f_6^6 f_2^{-2} \left[\frac{1}{2}(1 + |B|^2)\bar{\mathcal{C}} - \bar{B}\mathcal{C} \right] \star_\Sigma d\mathcal{C} + \text{c.c.} \tag{3.2.5}$$

The task at hand is to evaluate the various ingredients in this expression more explicitly. To evaluate the metric factors more explicitly we use the expressions in (3.1.7), which yields

$$f_6^6 f_2^{-2} = 54\,\mathcal{G}\left(\frac{1+R}{1-R}\right)^3 \ . \tag{3.2.6}$$

The pullback of $\star_\Sigma d\mathcal{C}$ to $\partial\Sigma$ does not involve ρ^2, and to evaluate it explicitly we note that $\partial\Sigma = \mathbb{R}$. It will be convenient for the explicit expansions to introduce real coordinates, $w = x + iy$, which yields

$$\star_\Sigma d\mathcal{C} = -(\partial_y \mathcal{C})dx \ . \tag{3.2.7}$$

Using eq. (3.2.6) and (3.2.7), the regularized on-shell action (3.2.5) becomes

$$S^{\mathrm{E}}_{\mathrm{IIB}} = -\frac{1}{64\pi G_{\mathrm{N}}} 54 \mathrm{Vol}_{\mathrm{AdS}_6,\mathrm{ren}} \mathrm{Vol}_{\mathrm{S}^2} \int_{\mathbb{R}} dx\, f^2 \mathcal{G} \left(\frac{1+R}{1-R}\right)^3 (\partial_y \mathcal{C}) \left(\frac{1}{2}(1+|B|^2)\bar{\mathcal{C}} - \bar{B}\mathcal{C}\right) + \text{c.c.}\,, \tag{3.2.8}$$

where the integrand is evaluated at $y = 0$. Close to the boundary we have $\kappa^2, \mathcal{G} \to 0$ and

$$R = 1 - \sqrt{\frac{6\kappa^2 \mathcal{G}}{|\partial_w \mathcal{G}|^2}} + \dots \ . \tag{3.2.9}$$

As discussed in sec. 5.5 of [48], $\mathcal{G}/(1-R)$ remains finite at the boundary and the same applies for f^2. We can thus simplify the on-shell action to

$$S^{\mathrm{E}}_{\mathrm{IIB}} = \frac{1}{8\pi G_{\mathrm{N}}} \mathrm{Vol}_{\mathrm{AdS}_6,\mathrm{ren}} \mathrm{Vol}_{\mathrm{S}^2} I_0 \ , \tag{3.2.10a}$$

$$I_0 = 54 \int_{\mathbb{R}} dx\, \frac{\mathcal{G}}{1-R} \times \frac{\partial_y \mathcal{C}}{(1-R)^2} \times \left(\bar{B} f^2 \mathcal{C} - \frac{2f^2-1}{2}\bar{\mathcal{C}}\right) + \text{c.c.}\ , \tag{3.2.10b}$$

where each factor in the integrand is finite separately on the real line.

To further evaluate the on-shell action in (3.2.10), we explicitly expand the composite

quantities κ^2, $\mathcal{G}$ as well as the actual supergravity fields around the real line, and it turns out that the subleading orders in the expansion play a crucial role. Since all the fields are determined from $\mathcal{A}_\pm$ we start by introducing a small y expansion for this functions, where we wrote $w = x + iy$. We have:

$$\mathcal{A}_\pm = D_\pm + \sum_{n=0}^{\infty} \frac{1}{n!}(iy)^n f_\pm^{(n)} \ , \qquad \partial_w \mathcal{A}_\pm = \sum_{n=0}^{\infty} \frac{1}{n!}(iy)^n f_\pm^{(n+1)} \ , \tag{3.2.11}$$

where for convenience we defined

$$f_\pm = \mathcal{A}_\pm^0 + \sum_{\ell=1}^{L} Z_\pm^\ell \ln|x - p_\ell| \ , \qquad D_\pm = i\pi \sum_{\ell=1}^{L} Z_\pm^\ell \Theta(p_\ell - x) \ , \tag{3.2.12}$$

and $f_\pm^{(n)} = (\partial_x)^n f_\pm$.

Simplifying the integrand of (3.2.10a) is a mere computation the details of which can be found in [4]. One finds:

$$S_{\text{IIB}}^{\text{E}} = -\frac{5}{3G_{\text{N}}} \text{Vol}_{\text{AdS}_6,\text{ren}} \text{Vol}_{\text{S}^2} \sum_{\substack{\ell,k,m,n=1 \\ \ell\neq k, m\neq n}}^{L} Z^{[\ell k]} Z^{[mn]} \int_{-\infty}^{p_\ell} dx \ \ln\left|\frac{x-p_k}{p_\ell - p_k}\right| \ln\left|\frac{x-p_m}{p_m - p_n}\right| \frac{1}{x-p_n} \ . \tag{3.2.13}$$

We note that the lower bound in the integral can be moved from $-\infty$ to $\min_\ell(p_\ell)$ due to $\sum_\ell Z_+^\ell = 0$. The integral can be solved explicitly and involves polylogarithms. While the result for generic configurations does not seem particularly illuminating, this allows us to get analytic results for particular solutions. We notice that the presence of the poles does not harm the integrability of the integrand: if we set $x = p_n + \epsilon$, where ϵ is real and $|\epsilon|$ small compared to 1 and to all $|p_k - p_\ell|$, we find that the integrand in (3.2.13) is $\mathcal{O}\big((\ln|\epsilon|)^2\big)$ and thus integrable across the pole. Note also that the $Z^{[\ell k]}$ are imaginary, so the expression (3.2.13) is manifestly real.

3.2.1 Scaling of the free energy

As shown in [50], the residues $Z_{\pm}^{\ell}$ of the differentials $\partial_w \mathcal{A}_{\pm}$ at the poles p_ℓ correspond to the charges of external 5-branes in brane-web constructions for 5d SCFTs. The details of the SCFT depend on the precise charge assignments, and the same applies for the free energy and, correspondingly, the gravitational on-shell action. Before coming to those details, we can address a more general question: how does the free energy scale under overall rescalings of the 5-brane charges?

To address this question we can assume to start with a generic solution to the regularity conditions in (3.1.6). Namely,

$$\mathcal{A}^0 Z_-^k + \bar{\mathcal{A}}^0 Z_+^k + \sum_{\ell \neq k} Z^{[\ell k]} \ln |p_\ell - p_k| = 0 \ . \tag{3.2.14}$$

We note that the equation is invariant under the following scaling

$$Z_+^\ell \to \gamma Z_+^\ell \ , \qquad Z_-^\ell \to \bar{\gamma} Z_-^\ell \ , \qquad \mathcal{A}^0 \to \gamma \mathcal{A}^0 \ , \qquad p_\ell \to p_\ell \ , \tag{3.2.15}$$

where we have allowed for $\gamma \in \mathbb{C}$. For the residues this simply amounts to a change of the overall complex normalization parametrized by σ in (3.1.2). So starting with a solution $(Z_{\pm}^{\ell}, \mathcal{A}^0, p_\ell)$ to the regularity conditions, a rescaling of this form produces another solution, and this precisely allows us to isolate the overall scale of the charges Z_+^ℓ. From (3.2.13) we immediately see that the on-shell action scales as

$$S_{\text{IIB}}^{\text{E}} \to |\gamma|^4 S_{\text{IIB}}^{\text{E}} \ . \tag{3.2.16}$$

For a real overall scaling by N, we thus obtain a free energy scaling as N^4. This is different from the N^2 scaling one would expect for the 't Hooft limit of a four dimensional Yang-Mills theory, and as exhibited by $\mathcal{N} = 4$ SYM and its $\text{AdS}_5 \times \text{S}^5$ dual. But this is

certainly not surprising, given the more exotic nature of the field theories described by 5-brane web constructions. It is also different from the $N^{5/2}$ scaling exhibited by the UV fixed points of 5d USp(N) gauge theories and their gravity duals [44]. As a curious aside, however, we note that the free energy for the orbifold quivers obtained from the USp(N) theories, which scales as $N^{5/2}k^{3/2}$, shows the same scaling if one naïvely sets $k = N$. As discussed in [50], there actually are classes of brane intersections described by the solutions discussed here which would naturally correspond to long quiver gauge theories with gauge groups of large rank, and we will discuss these examples in more detail in the next section.

3.2.2 Solutions with 3, 4 and 5 poles

We now evaluate the general expression for the free energy in (3.2.13) for classes of solutions with 3 up to 5 poles. It will be convenient to separate off the general overall factors as in (3.2.10a), and focus on the solution-specific part I_0.

3-pole solutions

We start with the 3-pole case. As discussed in sec. 4.1 of [50], the SL$(2,\mathbb{R})$ automorphisms of the upper half plane can be used to fix the position of all poles, which we once again choose as

$$p_1 = 1 \ , \qquad p_2 = 0 \ , \qquad p_3 = -1 \ . \tag{3.2.17}$$

The regularity conditions are solved by $\mathcal{A}^0 = \omega_0\lambda_0 s \ln 2$. The free parameters of the solutions are given by the residues, corresponding to the charges of the external 5-branes, subject to charge conservation. The integral I_0 in (3.2.10b) for a generic choice of residues evaluates to

$$I_0 = -80\pi\zeta(3)(Z^{[12]})^2 \ . \tag{3.2.18}$$

The on-shell action therefore is a simple function that is quartic in the residues, and manifestly invariant under the SU(1, 1) duality symmetry of type IIB supergravity since the $Z^{[\ell k]}$ are.[4] Note also that $Z^{[\ell k]}$ is imaginary, and I_0 positive. For the particular case of the "N-junction" [62], discussed in sec. 4.3 of [50] and realized by the charge assignment $Z^1_+ = N$, $Z^2_+ = iN$, we have $Z^{[12]} = 2iN^2$ and thus find the free energy quartic in N.

4-pole solutions

For solutions with four poles we can once again fix the position of three poles by $\mathrm{SL}(2,\mathbb{R})$, but the position of one pole remains a genuine parameter. It is fixed by the regularity conditions in (3.1.6) and thus becomes a non-trivial function of the residues. We therefore expect in general more interesting dependence on the charges compared to the 3-pole case. However, for the special class of 4-pole solutions discussed in sec. 4.2 of [50], where

$$Z^3_+ = -Z^1_+ \ , \qquad\qquad Z^4_+ = -Z^2_+ \ , \tag{3.2.19}$$

the position of the fourth pole is independent of the residues. In that case the regularity conditions are solved by

$$p_1 = 1 \ , \qquad p_2 = \frac{2}{3} \ , \qquad p_3 = \frac{1}{2} \ , \qquad p_4 = 0 \ , \tag{3.2.20}$$

along with $\mathcal{A}^0 = Z^2_+ \ln 3 - Z^1_+ \ln 2$. The position of all poles is therefore fixed regardless of the choice of charges, and we may again expect the on-shell action to be a simple quartic function of the residues. Indeed, the result for the integral is

$$I_0 = -280\pi\zeta(3)(Z^{[12]})^2 \ , \tag{3.2.21}$$

[4]The transformations spelled out in sec. 5.1 of [48] can be realized by transforming the residues as $Z^\ell_+ \to uZ^\ell_+ - vZ^\ell_-$ and $Z^\ell_- \to \bar{u}Z^\ell_- - \bar{v}Z^\ell_+$.

and of the same general form as the 3-pole result. We also note the factor $\zeta(3)$ appearing again. For the solutions discussed in sec. 4.2 of [50], with $-Z_+^1 = Z_+^3 = (1+i)N$ and $Z_+^2 = -Z_+^4 = (1-i)M$, we have $Z^{[12]} = 4iMN$. In particular, for $M = N$ the free energy again scales like N^4, a feature which we will come back to in the discussion.

We will now discuss a different configuration with 4 poles, for which the position of the fourth pole actually depends on the choice of charges. To this end, it is convenient to move the position of one pole off to infinity, which we will discuss here for a generic L-pole solution. To move the L-th pole p_L to infinity, we perform the following replacements and limit

$$p_L \to -\infty \ , \qquad\qquad \mathcal{A}_\pm^0 \to \tilde{\mathcal{A}}_\pm^0 = \mathcal{A}_\pm^0 - Z_\pm^L \ln|p_L| \ . \tag{3.2.22}$$

Note that the conjugation relation between the original integration constants, $\bar{\mathcal{A}}_\pm^0 = -\mathcal{A}_\pm^0$, holds in the same form for $\tilde{\mathcal{A}}_\pm^0$. In terms of the redefined integration constants, the expressions for the holomorphic functions then become

$$\mathcal{A}_\pm = \tilde{\mathcal{A}}_\pm^0 + \sum_{\ell=1}^{L-1} Z_\pm^\ell \ln(w - p_\ell) \ . \tag{3.2.23}$$

Note that this expression explicitly involves only $L-1$ poles and $L-1$ residues. These residues, however, are not constrained to sum to zero and the number of independent parameters is therefore unchanged. The conditions for $\mathcal{G} = 0$ on the boundary become

$$\tilde{\mathcal{A}}_+^0 Z_-^k - \tilde{\mathcal{A}}_-^0 Z_+^k + \sum_{\substack{\ell=1 \\ \ell\neq k}}^{L-1} Z^{[\ell k]} \ln|p_\ell - p_k| = 0 \ , \qquad\qquad k = 1, .., L-1 \ . \tag{3.2.24}$$

These are only $L-1$ conditions, as compared to L conditions previously. However, the sum does not manifestly vanish and the number of independent conditions therefore is also not modified. The class of 4-pole solutions with (3.2.19) can now be realized as

$$p_1 = 1 \ , \qquad\qquad p_2 = 0 \ , \qquad\qquad p_3 = -1 \ , \qquad\qquad \tilde{\mathcal{A}}_\pm^0 = 0 \ , \tag{3.2.25}$$

and computing the on-shell action reproduces (3.2.21).

The class of 4-pole solutions we wish to discuss next is parametrized by an overall scale n of the residues and an angle θ, and obtained by fixing

$$Z_+^1 = n \ , \qquad Z_+^2 = in \qquad Z_+^3 = ne^{i\theta} \ , \qquad Z_+^4 = -(1+i+e^{i\theta})n \ . \tag{3.2.26}$$

The position of three of the poles can once again be fixed arbitrarily, and we choose

$$p_1 = 1 \ , \qquad p_2 = 0 \ , \qquad p_4 \to -\infty \ . \tag{3.2.27}$$

This leaves the position of the third pole, p_3, along with the (complex) constant $\mathcal{A}^0$ to be determined from the conditions in (3.1.6). The resulting equation determining p_3 after solving for $\mathcal{A}^0$ is

$$Z^{[1,3]}Z^{[2,4]} \ln(1-p_3)^2 = Z^{[1,4]}Z^{[2,3]} \ln p_3^2 \ . \tag{3.2.28}$$

Note that n drops out of this equation and p_3 therefore depends on θ only. We take the position of the pole as parameter and solve for θ, which can be done in closed form and yields four branches of solutions. The criterion for the choice of branch is that θ should be real and the zeros s_n in the upper half plane. The explicit expressions are bulky and not very illuminating, and we show a plot of θ as function of p_3 in fig. 3.1 instead.

Since p_3 is independent of n, the on-shell action depends on n only through an overall factor n^4, as expected from the scaling analysis in sec. 3.2.1. The dependence on θ, however, is non-trivial and we show the result in fig. 3.1. We note the presence of three minima, which all correspond to the 4-pole solution degenerating to a 3-pole solution: for $\theta \to 0$ we have $Z_+^3 \to Z_+^1$ and $p_3 \to p_1$, for $\theta \to \pi/2$ we have $Z_+^3 \to Z_+^2$ and $p_3 \to p_2$, and for $\theta \to 5\pi/4$ we have $Z_+^3 \to (1+\sqrt{2})Z_+^4$ and $p_3 \to p_4$. That means in all these cases two poles coalesce and their residues add. The free energy coincides with that of the resulting 3-pole configuration.

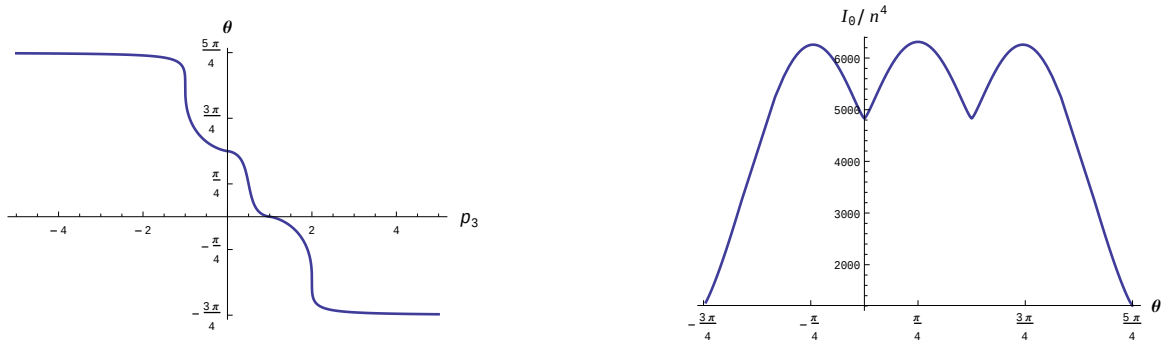

Figure 3.1: The left hand side shows θ as function of p_3, for the 4-pole solution with residues given in eq. (3.2.26). The right hand side shows I_0, which via (3.2.10) corresponds to the on-shell action.

The 3-pole configurations resulting from $\theta \to 0$ and $\theta \to \pi/2$ have two charges with the same moduli and the same relative phase up to a sign. Since the formula in (3.2.18) is insensitive to these differences, this explains the coincident free energies. It is intriguing to observe that the value of the free energy assumes a local minimum for all the cases where the solution reduces to a 3-pole configuration. The sphere free energy in odd dimension can be used as a measure for the number of degrees of freedom, and one may speculate that splitting one pole into two, or equivalently one external 5-brane into two, will generically increase that number. While certainly true for this specific example, it is an interesting open question whether this behavior holds more generally.

5-pole solutions

As a final example we will consider a class of solutions with five poles. In general we now have two positions of the poles depending on the choice of residues, but we will focus on a class of solutions which are parametrized by only two real numbers, with residues given by

$$Z_+^1 = -Z_+^3 = M \ , \qquad Z_+^2 = 2iN \ , \qquad -Z_+^4 = iZ_+^5 = (1+i)N \ . \tag{3.2.29}$$

The corresponding 5-brane intersection is shown in fig. 3.2.

As before three poles can be fixed by $\mathrm{SL}(2,\mathbb{R})$ and we resort to the choice in (3.2.17).

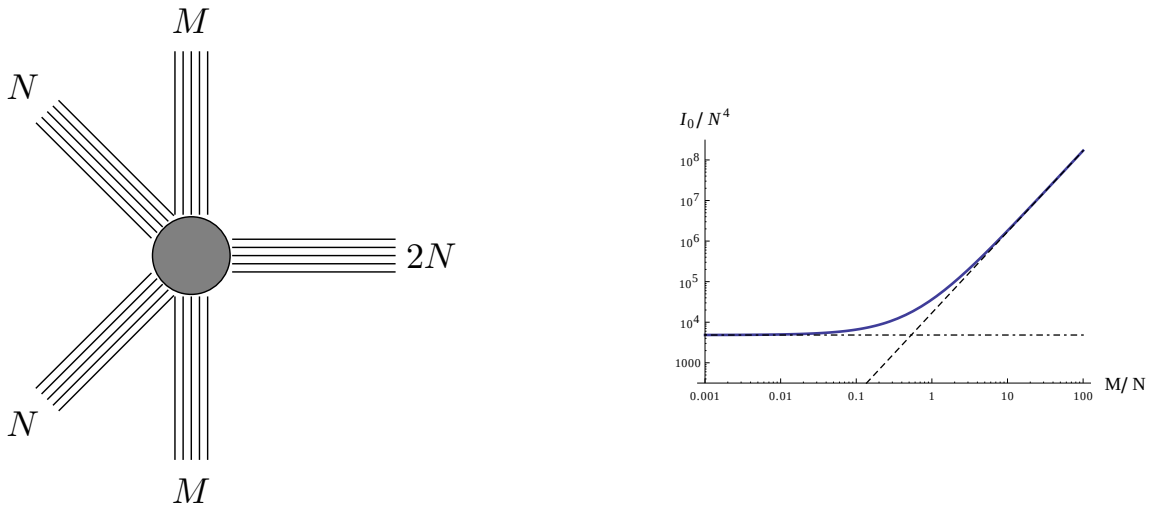

Figure 3.2: The left hand side shows a 5-brane intersection corresponding to the charges in (3.2.29). On the right hand side is a log-log plot of I_0 for the 5-pole solution with residues given in (3.2.29). Via (3.2.10) this corresponds to the on-shell action, as function of M/N. The constant dot-dashed line shows $80\pi\zeta(3)\cdot 16N^4$, which, via (3.2.18), is the value of I_0 for the 3-pole solution resulting from (3.2.29) for $M=0$. The dashed line shows $280\pi\zeta(3)\cdot 16M^2N^2$, which, via (3.2.21), is I_0 for a 4-pole solution with $-Z^1_+ = Z^3_+ = 2iN$ and $Z^2_+ = -Z^4_+ = M$.

The regularity conditions in (3.1.6) are solved by

$$p_5 = -p_4 \ , \qquad\qquad A^0 = iN\log|p_4^2-1| \ , \tag{3.2.30}$$

where p_4 is determined by the equation

$$(M-N)\log(p_4-1)^2 - (M+N)\log(p_4+1)^2 + N\log 16 = 0 \ . \tag{3.2.31}$$

The choice of residues can be realized via (3.1.5), by fixing $\sigma = -2iNp_4^2/(s_1s_2s_3)$ and the zeros s_1, s_2, s_3 as the three solutions to the cubic equation

$$isM(s^2-p_4^2) + p_4N(s^2-1)(p_4-is) = 0 \ . \tag{3.2.32}$$

To solve (3.2.31) it is once again convenient to fix p_4 and determine the resulting ratio M/N. We choose $p_4 \leq -\sqrt{5}$, which produces zeros in the upper half plane and positive M/N. The

on-shell action divided by N^4, as function of the ratio M/N, is shown in fig. 3.2. We clearly see that the dependence on M/N is not simply quadratic, which we would have expected if the position of the poles had not depended on M/N. Instead, I_0/N^4 interpolates between approaching a constant for small M/N and quadratic dependence for large M/N.

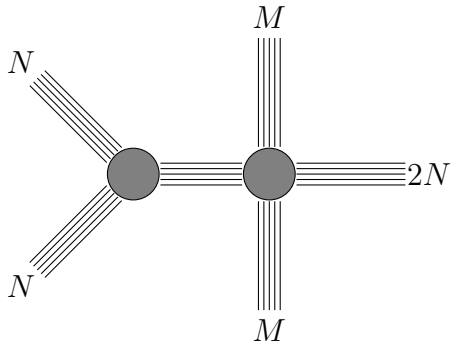

Figure 3.3: Global deformation (in the classification of [39,40]) of the brane intersection shown in the left hand side of fig. 3.2, corresponding to a relevant deformation of the dual SCFT.

The asymptotic behavior for $M/N \to 0$ and $M/N \to \infty$ can be understood in more detail as follows. For $M \to 0$, we expect the solution to reduce to a 3-pole configuration, since two of the residues in (3.2.29) vanish. Indeed, in that limit two of the zeros s_n approach the real line and annihilate the poles p_1, p_3. With one zero remaining in the interior of the upper half plane and three poles on the real line, we indeed find a regular 3-pole configuration. Correspondingly, the on-shell action as shown in fig. 3.2 for $M/N = 0$ agrees with (3.2.18) evaluated with the remaining residues. For large M/N, the behavior is not quite as immediately clear from the form of the residues. But we can gain some intuition from looking at deformations of the web. The solutions we are considering here describe the conformal phase of the dual SCFTs, where in the brane construction all external branes intersect at one point. Deformations of the web where the external branes are moved correspond to relevant deformations of the dual SCFT [39, 40], and a particular example is shown in fig. 3.3. We may view it as gluing an intersection of M NS5-branes and $2N$ D5-branes with an SL(2,$\mathbb{R}$) rotated version of the "N-junction". For large M, it suggests that the structure of the web is dominated by the intersection of M NS5-branes and $2N$ D5-branes. The number of degrees

of freedom provided by the "extra vertex" compared to the 4-brane intersection of NS5 and D5-branes does not appear to scale with M, and we therefore expect the free energy of the 5-pole solution at large M/N to approach the free energy of a 4-pole solution with charges corresponding to M NS5 and $2N$ D5-branes. As shown in fig. 3.2, this is indeed the case.

3.3 Entanglement entropy

In this section we use the Ryu-Takayanagi prescription [7] to compute holographic entanglement entropies for the 5d SCFTs dual to the supergravity solutions. The main parts of the derivation will hold for a generic choice of the region for which we compute the entanglement entropy, as we will explain shortly, but our main interest is in regions of spherical shape.

The entanglement entropy is given by the area of a codimension-2 surface, anchored at a fixed time on the boundary of AdS_6 such that it coincides with the entangling surface. For a generic choice of entangling surface, we thus have to compute the area of an eight-dimensional surface γ_8 wrapping S^2 and Σ, and which is of codimension 2 in AdS_6. The resulting expression for the entanglement entropy reads

$$S_{\mathrm{EE}} = \frac{\mathrm{Area}(\gamma_8)}{4G_{\mathrm{N}}} = \frac{1}{4G_{\mathrm{N}}} \int_{\gamma_8} \mathrm{vol}_{\gamma_8} \ . \tag{3.3.1}$$

The volume form reduces to

$$\mathrm{vol}_{\gamma_8} = f_6^4 f_2^2 \, \mathrm{vol}_{\gamma_4} \wedge \mathrm{vol}_{\mathrm{S}^2} \wedge \mathrm{vol}_{\Sigma} \ , \tag{3.3.2}$$

where γ_4 is the codimension-2 minimal surface in a unit radius AdS_6 which is anchored at the conformal boundary and ends there on the entangling surface. The computation of S_{EE} as a result simplifies to

$$S_{\mathrm{EE}} = \frac{1}{4G_{\mathrm{N}}} \mathrm{Vol}_{\mathrm{S}^2} \cdot \mathcal{J} \cdot \mathrm{Area}(\gamma_4) \ , \tag{3.3.3}$$

where Area(γ_4) is the area of the four-dimensional minimal surface in AdS_6 and with $g_\Sigma = 4\rho^2|dw|^2$ we have

$$\mathcal{J} = 4\int_\Sigma d^2w f_6^4 f_2^2 \rho = \frac{8}{3}\int_\Sigma d^2w\ \kappa^2\mathcal{G} = \frac{8}{3}\int_\Sigma d^2w(\partial_{\bar{w}}\mathcal{G})\partial_w\mathcal{G}\ . \tag{3.3.4}$$

We note in particular that, due to the factorization in (3.3.3), once $\mathcal{J}$ is known the computation of entanglement entropies reduces to the analogous computation in AdS_6.

One can explicitly evaluates the integrand of $\mathcal{J}$ in terms of the parameters of the problem. Making use of the explicit expressions for $\mathcal{A}_\pm$ and of the regularity conditions (3.1.6) we find

$$\mathcal{J} = -\frac{8}{3}\sum_{\substack{\ell,k,m,n=1\\ \ell\neq k, m\neq n}}^{L} Z^{[\ell k]}Z^{[mn]}\int_\Sigma d^2w \ln\left|\frac{w-p_\ell}{p_k-p_\ell}\right|^2 \ln\left|\frac{w-p_m}{p_m-p_n}\right|^2 \frac{1}{\bar{w}-p_n}\frac{1}{w-p_k}\ . \tag{3.3.5}$$

This expression becomes manifestly real upon symmetrizing the integrand under the exchange of the index pairs (ℓ,k) and (m,n), which are independently summed over. In addition, using charge conservation, one can show that the combination $dw\partial_w\mathcal{G}$ is invariant under SL(2,$\mathbb{R}$) transformations

$$w \to \frac{aw+b}{cw+d}\ , \qquad\qquad p_k \to \frac{ap_k+b}{cp_k+d}\ , \tag{3.3.6}$$

with $ad-bc=1$. The expression for $\mathcal{J}$ in (3.3.4) is therefore SL(2,$\mathbb{R}$) invariant, as expected, and we can again fix the location of three poles at arbitrary positions.

3.3.1 Spherical regions

For the specific case of a spherical entangling surface of radius r_0 at a fixed $t = t_0$, we just have to evaluate the area of the corresponding minimal surface in an AdS_6 of unit radius.

we choose coordinates in AdS_6 such that

$$ds^2_{\mathrm{AdS}_6} = \frac{dz^2 - dt^2 + dr^2 + r^2 d\Omega^2_{S^3}}{z^2} \ . \tag{3.3.7}$$

The minimal surface can be parametrized by $r = r(z)$ and its area is given by

$$\mathrm{Area}(\gamma_4) = \mathrm{Vol}_{\mathrm{S}^3} \int dz \frac{r(z)^3 \sqrt{1 + r'(z)^2}}{z^4} \ . \tag{3.3.8}$$

Extremizing this functional yields the usual solution

$$r(z) = \sqrt{r_0^2 - z^2} \ . \tag{3.3.9}$$

The z integral is divergent at $z = 0$. Although holographic renormalization for submanifolds is well understood [63], the divergences in the entanglement entropy are usually kept, as a reflection of the short-distance behavior of QFTs. The universal part in odd dimensions, however, is the finite contribution and for the surfaces considered here given by

$$\mathrm{Area}_{\mathrm{ren}}(\gamma_4) = \frac{2}{3} \mathrm{Vol}_{\mathrm{S}^3} \ . \tag{3.3.10}$$

In summary, the entanglement entropy for a spherical region is given by the expression in (3.3.3), with the universal part of the area of the minimal surface in (3.3.10) and $\mathcal{J}$ given in (3.3.5). We note that this expression manifestly exhibits the same scaling with the residues Z^ℓ_+, corresponding to the charges of the external 5-branes, as the expression for the on-shell action in (3.2.13).

3.3.2 Matching to free energy

In this section we show that for all the examples discussed in sec. 3.2.2 the finite part of the holographic entanglement entropy for a spherical region is equal to minus the finite part of

the free energy on S^5. To accomplish this we will reduce part of the two-dimensional integral over Σ appearing in equation (3.3.4) to a one-dimensional integral over the real line which has the same form as the one-dimensional integral appearing in the on-shell action (3.2.13), and show that the remaining part vanishes.

Using $\kappa^2 = -\partial_w \partial_{\bar{w}} \mathcal{G}$ and the definition of $\mathcal{G}$ in (3.1.4), the integral $\mathcal{J}$ given in (3.3.4) can be rewritten as

$$\mathcal{J} = -\frac{8}{3} \int_\Sigma d^2w \, \partial_w \partial_{\bar{w}} \mathcal{G} \left(|\mathcal{A}_+|^2 - |\mathcal{A}_-|^2 + \mathcal{B} + \bar{\mathcal{B}} \right) \ . \tag{3.3.11}$$

We split $\mathcal{J}$ into two terms:

$$\mathcal{J} = \mathcal{J}_1 + \mathcal{J}_2 \ , \tag{3.3.12a}$$

$$\mathcal{J}_1 = -\frac{4}{3} \int_\Sigma d^2w \, \partial_w \partial_{\bar{w}} \mathcal{G} \left(\mathcal{B} + \bar{\mathcal{B}} \right) \ , \tag{3.3.12b}$$

$$\mathcal{J}_2 = -\frac{8}{3} \int_\Sigma d^2w \, \partial_w \partial_{\bar{w}} \mathcal{G} \left(|\mathcal{A}_+|^2 - |\mathcal{A}_-|^2 + \frac{1}{2} \left(\mathcal{B} + \bar{\mathcal{B}} \right) \right) \ . \tag{3.3.12c}$$

First we evaluate $\mathcal{J}_1$ and will argue below that the second integral $\mathcal{J}_2$ vanishes. Using the holomorphicity of $\mathcal{B}$ one can rewrite $\mathcal{J}_1$ at first as a sum of total derivatives and then as a line integral over the real line. Using the explicit expressions for $\mathcal{A}_\pm$ we find:

$$\mathcal{J}_1 = -\frac{8\pi}{3} \sum_{\substack{\ell,k,m,n=1 \\ \ell \neq k, m \neq n}}^{L} \int_{-\infty}^{\infty} dx \frac{Z^{[\ell k]} Z^{[mn]}}{x - p_n} \ln \left| \frac{x - p_m}{p_m - p_n} \right| \ln \left| \frac{x - p_k}{p_k - p_\ell} \right| \Theta \left(p_\ell - x \right) \ . \tag{3.3.13}$$

Plugging this result into (3.3.3) gives the following contribution to the entanglement entropy

$$S_{\text{EE1}} = -\frac{4\pi}{9 G_N} \text{Vol}_{S^2} \text{Vol}_{S^3} \sum_{\substack{\ell,k,m,n=1 \\ \ell \neq k, m \neq n}}^{L} Z^{[\ell k]} Z^{[mn]} \int_{-\infty}^{p_\ell} dx \ln \left| \frac{x - p_m}{p_m - p_n} \right| \ln \left| \frac{x - p_k}{p_k - p_\ell} \right| \frac{1}{x - p_n} \ . \tag{3.3.14}$$

We can compare this result with the value of the finite part of the on-shell action derived in

section 3.2:

$$(S^{\rm E}_{\rm IIB})^{\rm finite} = \frac{8}{9G_{\rm N}}{\rm Vol}_{\rm S^5}{\rm Vol}_{\rm S^2}\sum_{\substack{\ell,k,m,n=1\\ \ell\neq k,m\neq n}}^{L} Z^{[\ell k]}Z^{[mn]}\int_{-\infty}^{p_\ell} dx\,\ln\left|\frac{x-p_k}{p_\ell-p_k}\right|\ln\left|\frac{x-p_m}{p_m-p_n}\right|\frac{1}{x-p_n}\ . \tag{3.3.15}$$

Inserting the expressions for the volumes of the 2-, 3- and 5-sphere given by

$${\rm Vol}_{\rm S^2} = 4\pi\ , \qquad {\rm Vol}_{\rm S^3} = 2\pi^2\ , \qquad {\rm Vol}_{\rm S^5} = \pi^3\ , \tag{3.3.16}$$

confirms the equality of the finite parts of the entanglement entropy and the on-shell action

$$(S_{\rm EE1})^{\rm finite} = -(S^{\rm E}_{\rm IIB})^{\rm finite}\ . \tag{3.3.17}$$

What remains to be shown is that the integral $\mathcal{J}_2$ vanishes and hence $S_{\rm EE1}$ given in (3.3.14) is the complete expression for the finite part of the entanglement entropy. The integral $\mathcal{J}_2$ given in (3.3.12c) can be written explicitly as

$$\mathcal{J}_2 = -\frac{4}{3}\sum_{\substack{\ell,k,m,n=1\\ \ell\neq k,m\neq n}}^{L} Z^{[mn]}Z^{[\ell k]}\int_\Sigma d^2w\,\frac{1}{\bar w-p_m}\Bigg(\ln\left|\frac{w-p_\ell}{p_k-p_\ell}\right|^2\ln\left|\frac{w-p_n}{p_m-p_n}\right|^2\frac{1}{w-p_k} + \ln\frac{w-p_\ell}{|p_k-p_\ell|}\ln\frac{\bar w-p_k}{|p_k-p_\ell|}\frac{1}{w-p_n}\Bigg)\ . \tag{3.3.18}$$

For the three-pole solutions we have shown analytically that this term vanishes, and for the four and five pole solutions discussed in sec. 3.2.2 we have verified this numerically. For all these cases we therefore find that the finite parts of the entanglement entropy and the on-shell action are related as expected on general grounds [34]. Although we do not currently have an analytic proof, this certainly suggests that the relation between free energy and entanglement entropy holds for all the solutions reviewed in sec. 3.1.

3.4 Discussion

We have studied the free energy of the field theories described by the supergravity solutions constructed in [49, 50]. Unlike for previously known AdS_6 solutions in type IIA supergravity, the computation of the free energy is straightforward albeit technically non-trivial for these solutions. We conclude that the isolated singularities that are present are mild and do not obstruct holographic computations. Moreover, the computation of the free energy via the entanglement entropy of a spherical region reproduces the result of the direct computation, a relation which is expected to hold on general grounds but corresponds to non-trivial integral identities in the explicit solutions considered here. These results support the interpretation of the solutions as holographic duals to the five-dimensional superconformal field theories engineered in type IIB string theory via 5-brane webs, and give first quantitative indications on the nature of the dual field theories. We will close with a more detailed discussion of the implications and reference to recent developments.

An immediate question concerning the supergravity solutions and their interpretation concerns the external 5-branes. In [49, 50] the singularities located at the poles were interpreted as the remnants of the external (p, q) five branes in the brane web construction of the five dimensional field theories, which flow to the dual SCFT in the conformal limit.

Whether brane webs with parallel external branes lead to well-defined five-dimensional SCFTs was initially questioned, with one potential obstacle being light states on the parallel branes that may not decouple from the field theory on the intersection. It was later argued that these light states do in fact decouple [43], and webs with parallel external branes indeed lead to well-defined 5d field theories after factoring out the decoupled states [64–68].

For our supergravity solutions this immediately poses the question of whether or not they include contributions from parallel external branes, e.g. in the form of states localized around the poles on $\partial\Sigma$. The computation of the free energy in sec. 3.2 and 3.3 indicates that this may not be the case: In both cases we could introduce a cut-off around the poles

on Σ and effectively remove them from the geometry. If states localized around the poles would contribute, we would expect the free energy to change by a finite amount, i.e. we would expect to produce non-trivial boundary terms. The scaling analysis for both cases shows that this is not the case, and we therefore do not seem to see contributions from the external 5-branes.

Another open question about the solutions was whether and how the external 5-branes end on 7-branes. We discussed in [50] that there was no indication for the presence of 7-branes and that a natural expectation would be that the supergravity solutions describe brane webs with only 5-branes. But with only access to the intersection, the possibility that external 7-branes would just not be directly accessible from the supergravity solution remained a valid option. Another natural option could then be that all 5-branes within a given stack of external 5-branes end on the same 7-brane. This allows for a brane web realization of the USp(N) theory which was initially engineered in type IIA string theory [43]. Our results for the free energy and entanglement entropy, however, disfavor this option: The scaling of the free energy in the USp(N) theory is $N^{5/2}$, which is different from the scaling in the 4-pole type IIB supergravity solutions discussed in sec. 3.2. In particular, the solutions with $Z^1_+ = -Z^3_+ = (1+i)N$ and $Z^2_+ = -Z^4_+ = (-1+i)N$, if all external branes within a given stack would end on the same 7-brane, would realize the USp(N) theory. But the scaling we find is N^4 instead of $N^{5/2}$. This suggests that the dual SCFTs may rather be of the long quiver type, as discussed in [50].

Finally, our results for the free energy in specific examples provide a clear target for field-theory computations. This result was recently replicated on the field theory side in [69], where the authors computed the sphere partition function numerically using supersymmetric localization.

Chapter 4

Type IIB 7-branes in warped AdS_6: partition functions, brane webs and probe limit

The space of 5d SCFTs that can be realized in Type IIB string theory can be extended substantially by adding additional 7-branes into 5-brane webs [41], and many insights have been obtained through the inclusion of 7-branes and in particular their associated branch cuts [62, 68, 70–73]. This motivates a corresponding extension of the construction of supergravity solutions. In [74] the construction of supergravity solutions has indeed been extended to incorporate punctures with non-trivial $SL(2,\mathbb{R})$ monodromy, signaling the presence of additional 7-branes. However, while the map between supergravity solutions and 5-brane webs appeared very clearly and naturally in the case without monodromy, where a given 5-brane intersection is entirely characterized by the charges of the external 5-branes, a corresponding map is less automatic in the case with additional 7-branes. This is largely due to the fact that 7-branes introduce a number of additional parameters, as we will review shortly and in more detail in sec. 4.1, and the fact that the analysis of the supergravity solutions is technically more challenging. This motivates further study of the solutions with monodromy, to

substantiate and clarify their interpretation.

As reviewed in section 3.1, the solutions in [74] are constructed in terms of two locally holomorphic functions $\mathcal{A}_\pm$ on the Riemann surface Σ, which is a disc or equivalently the upper half plane. The differentials of these functions have common poles on the boundary of Σ, at which the entire solution approaches that for a (p, q) 5-brane, as constructed in [59], with $p - iq$ identified with the residue at the pole. This facilitates the identification of the solutions with (p, q) 5-brane webs. For solutions with monodromy, the differentials in addition have a number of branch points in the interior of Σ with associated branch cuts, across which the supergravity fields undergo a parabolic $SL(2, \mathbb{R})$ transformation. The regularity conditions for the supergravity solutions as constructed in [74] constrain each puncture to lie on a curve in Σ. This leaves one real parameter in addition to the orientation of the branch cut for a puncture with fixed monodromy. Adding a 7-brane into a 5-brane web correspondingly adds new parameters. In addition to the orientation of the branch cut, there is a choice of which face of the web the 7-brane is placed in. This choice remains meaningful in the conformal limit and naturally turns into a continuous parameter in a "large-N" limit, thus providing a potential brane web realization of the supergravity parameter. One may wonder, however, whether a given puncture corresponds to an isolated 7-brane in a certain face of the web, or whether 5-branes are attached to it. Similarly, one may wonder whether solutions with punctures at different points in Σ can be related by 7-brane moves with the associated Hanany-Witten brane creation effect [75], or whether punctures at different points correspond to genuinely different brane webs. An unambiguous brane web interpretation for the solutions constructed in [74] is therefore not immediately clear. In this chapter, based on [5], we will expand on the interpretation of the solutions in [74] in several ways and address these questions. We will constrain the monodromy around the punctures to realize the $SL(2, \mathbb{R})$ transformation appropriate for D7 branes for simplicity, but the results immediately generalize to other 7-branes by globally conjugating with suitable $SL(2, \mathbb{R})$ elements.

4.1 Review of warped $\mathbf{AdS}_6 \times \mathbf{S}^2 \times \Sigma$ solutions with monodromy

We will now briefly review the construction to add punctures with monodromy to the solutions without monodromy summarized in section 3.1. We will exclusively focus on punctures with D7-brane monodromy in this chapter, and refer to [74] for the more general case. Note, however, that with no restrictions on the residues at the poles on $\partial\Sigma$, the case of punctures with generic (commuting) parabolic $SL(2,\mathbb{R})$ monodromies can be obtained straightforwardly from the results presented here by global $SL(2,\mathbb{R})$ transformations. In that sense the restriction to D7-brane monodromy is without loss of generality.

In addition to the parameters for the solutions without monodromy, a solution with D7-brane punctures depends on the loci of the punctures, w_i, $i = 1, \ldots, I$, a real number n_i for each puncture and a phase γ_i specifying the orientation of the branch cut. From this data one constructs a function f, which encodes the branch points and branch cut structure, via

$$f(w) = \sum_{i=1}^{I} \frac{n_i^2}{4\pi} \ln\left(\gamma_i \frac{w - w_i}{w - \bar{w}_i}\right) \ . \tag{4.1.1}$$

With the help of this function and $Y^\ell \equiv Z_+^\ell - Z_-^\ell$, the locally holomorphic functions for a solution with monodromy are expressed as

$$\mathcal{A}_\pm = \mathcal{A}_\pm^0 + \sum_{\ell=1}^{L} Z_\pm^\ell \ln(w - p_\ell) + \int_\infty^w dz\ f(z) \sum_{\ell=1}^{L} \frac{Y^\ell}{z - p_\ell} \ , \tag{4.1.2}$$

again with $\bar{\mathcal{A}}_\pm^0 = -\mathcal{A}_\mp^0$. The contour for the integration is chosen such that it does not cross any of the branch cuts. Once the functions $\mathcal{A}_\pm$ are specified the other fields can be derived using the same equations of section 3.1. The regularity constraints that the parameters have

to satisfy for the solutions with D7-brane monodromy are

$$0 = 2\mathcal{A}^0_+ - 2\mathcal{A}^0_- + \sum_{\ell=1}^{L} Y^\ell \ln|w_i - p_\ell|^2 \ , \qquad i = 1, \cdots, I \ , \tag{4.1.3}$$

$$0 = 2\mathcal{A}^0_+ \mathcal{Y}^k_- - 2\mathcal{A}^0_- \mathcal{Y}^k_+ + \sum_{\ell \neq k} Z^{[\ell,k]} \ln|p_\ell - p_k|^2 + Y^k J_k \ , \qquad k = 1, \cdots, L \ . \tag{4.1.4}$$

With $\mathcal{S}_k \subset \{1, \cdots, I\}$ denoting the set of branch points for which the associated branch cut intersects the real line in the interval (p_k, ∞), J_k is given by

$$J_k = \sum_{\ell=1}^{L} Y^\ell \left[\int_\infty^{p_k} dx f'(x) \ln|x - p_\ell|^2 + \sum_{i \in \mathcal{S}_k} \frac{in_i^2}{2} \ln|w_i - p_\ell|^2 \right] . \tag{4.1.5}$$

The residues of the differentials of (4.1.2) at the poles are given by

$$\mathcal{Y}^\ell_\pm = Z^\ell_\pm + f(p_\ell) Y^\ell \ . \tag{4.1.6}$$

It is these residues that translate to the charges of the external 5-branes and replace the Z^ℓ_+ in (3.1.10), resulting in

$$(q_1 - iq_2)Q = \frac{8}{3} \mathcal{Y}^m_+ \ . \tag{4.1.7}$$

4.2 Match to probe D7 branes and κ-symmetry

In this section we study probe D7 branes embedded into the solutions reviewed in sec. 3.1, subject to the requirement that they preserve all bosonic and fermionic symmetries of the background. This is motivated by the fact that the solutions with and without punctures discussed in sec. 3.1 are both invariant under $SO(2,5) \oplus SO(3)$ and sixteen supersymmetries. The requirement to preserve the bosonic symmetries forces the D7-branes to wrap the entire $\mathrm{AdS}_6 \times \mathrm{S}^2$ part of the geometry, and the entire embedding is therefore characterized by the point at which the D7-branes are localized in Σ. The choice of coordinates on AdS_6 is

irrelevant for the analysis, and we will therefore leave it general. The worldvolume metric induced by the string-frame background metric on the D7-brane reads

$$g = \tilde{f}_6(w,\bar{w})^2 ds^2_{\mathrm{AdS}_6} + \tilde{f}_2(w,wb)^2 ds^2_{\mathrm{S}^2} \ , \tag{4.2.1}$$

where the tilde denotes that the radii are in string frame. The pullback of the ten-dimensional frame to the D7-brane, E^a, is given by

$$\begin{aligned} E^m &= \tilde{f}_6 \hat{e}^m \ , & m &= 0,\ldots,5 \ , \\ E^i &= \tilde{f}_2 \hat{e}^i \ , & i &= 6,7 \ , \\ E^8 &= E^9 = 0 \ , \end{aligned} \tag{4.2.2}$$

where $\hat{e}^m$ and $\hat{e}^i$ denote the canonical frames for AdS_6 and S^2, respectively. The symmetry requirement constrains the field strength of the worldvolume gauge field, F, to be proportional to the volume form of S^2, and we can thus parametrize it as

$$F = \mathcal{K}\, \mathrm{vol}_{\mathrm{S}^2} \ , \tag{4.2.3}$$

where $\mathrm{vol}_{\mathrm{S}^2}$ is the canonical volume form on S^2 of unit radius and $\mathcal{K}$ is a real constant to be solved for for each supersymmetric embedding.

4.2.1 κ-symmetry and $SU(1,1)/U(1)$

The supersymmetries preserved by a probe brane embedding are those generated by background Killing spinors ϵ that are compatible with the κ-symmetry condition

$$\Gamma_\kappa \epsilon = \epsilon \ , \tag{4.2.4}$$

where Γ_κ is a projector that depends on the embedding and has been constructed in [76–78]. The condition will provide constraints on the background fields, that single out the locations where probe branes can be added while preserving supersymmetry. The explicit expression for Γ_κ is given by

$$\Gamma_\kappa = \frac{1}{\sqrt{\det(1+X)}} \sum_{n=0}^{\infty} \frac{1}{2^n n!} \gamma^{j_1 k_1 \dots j_n k_n} X_{j_1 k_1} \dots X_{j_n k_n} J^{(n)}_{(p)} \ , \tag{4.2.5}$$

where the $\gamma_\mu \equiv E^a_\mu \Gamma_a$ are the pullback of the background Clifford algebra generators to the 7-brane worldvolume, $X^i_{\ j} \equiv g^{ik}\mathcal{F}_{kj}$, g is the metric induced on the worldvolume by the string-frame background metric, and $\mathcal{F}$ is defined in terms of the worldvolume field strength F and the background NS-NS two-form field B_2 as

$$\mathcal{F} = F - B_2 \ . \tag{4.2.6}$$

For $J^{(n)}_{(p)}$ we will use the conventions for complex spinors as spelled out in sec. 2.2 of [79], such that

$$J^{(n)}_{(p)}\epsilon = i(-1)^{(p-1)/2} \begin{cases} \Gamma_{(0)}\epsilon & n + (p-3)/2 \text{ even} \\ C\left(\Gamma_{(0)}\epsilon\right)^\star & n + (p-3)/2 \text{ odd} \end{cases} , \tag{4.2.7}$$

with $\Gamma_{(0)}$ given by

$$\Gamma_{(0)} = \frac{1}{(p+1)!\sqrt{-\det g}}\, \varepsilon^{i_1 \dots i_{p+1}} \gamma_{i_1 \dots i_{p+1}} \ . \tag{4.2.8}$$

We note in particular that Γ_κ is not a $\mathbb{C}$-linear operator, which will play a role shortly.

A crucial subtlety in the formulation of the κ-symmetry conditions in the backgrounds we are interested in arises due to the presence of non-trival axion-dilaton backgrounds. The κ-symmetry conditions derived in [76–78] and the supergravity solutions in [48–50, 74] are both formulated in terms of the physical axion and dilaton fields. This amounts to passing

from the formulation of type IIB supergravity in [57, 58], with linear $SU(1,1)$ action and $U(1)$ gauge symmetry, to gauge-fixed versions. In the notation used in sec. 2 of [48], the covariant formulation in particular involves a complex one-form P, which is constrained by Bianchi identities and transforms under the $U(1)$ as

$$P \to e^{2i\theta} P \ . \tag{4.2.9}$$

Crucially for the κ-symmetry analysis, the generators of (local) supersymmetries transform under this $U(1)$ as

$$\epsilon \to e^{i\theta/2} \epsilon \ . \tag{4.2.10}$$

Expressing P and Q in terms of physical fields was done in [48] by the following choice for P

$$P = \frac{dB}{1-|B|^2} \ , \qquad\qquad B = \frac{1+i\tau}{1-i\tau} \ . \tag{4.2.11}$$

In contrast, as discussed in sec. 3 of [77], the expression used for the derivation of the κ-symmetry condition is

$$P_\kappa = \frac{d\tau}{\bar{\tau}-\tau} \ . \tag{4.2.12}$$

These two choices are related by a $U(1)$ transformation as follows

$$P = e^{2i\theta_\kappa} P_\kappa \ , \qquad\qquad e^{2i\theta_\kappa} = \frac{1+i\bar{\tau}}{1-i\tau} \ . \tag{4.2.13}$$

Consequently, the background Killing spinors used in the κ symmetry condition have to be transformed according to (4.2.10) to get the condition in the conventions used for the supergravity solutions. Since Γ_κ is in general not a $\mathbb{C}$-linear operator, this modifies the

condition in a non-trivial way. We multiply (4.2.4) by $e^{i\theta_\kappa/2}$, and may then state the converted condition as follows: The supersymmetries preserved by a probe brane embedding in the solutions of [48–50, 74] are those generated by Killing spinors compatible with

$$\Gamma_\kappa \epsilon = \epsilon \ , \tag{4.2.14}$$

where Γ_κ is as given in (4.2.5) and

$$J^{(n)}_{(p)}\epsilon = i(-1)^{(p-1)/2} \begin{cases} \Gamma_{(0)}\epsilon & n+(p-3)/2 \text{ even} \\ e^{i\theta_\kappa} C \left(\Gamma_{(0)}\epsilon\right)^\star & n+(p-3)/2 \text{ odd} \end{cases} , \tag{4.2.15}$$

with $\Gamma_{(0)}$ as given in (4.2.8) and ϵ in 4.2.14 referring to spinors in the supergravity conventions of [48–50, 74]. We note that the phase $e^{i\theta_\kappa}$ occured for similar reasons in the (re)definition of the three-form field in [80].

4.2.2 BPS equations for D7-branes

We now turn to the specific case of probe D7 branes wrapping $\mathrm{AdS}_6 \times \mathrm{S}^2$. We identify the NS-NS two-form field B_2 and the R-R two-form potential $C_{(2)}$ with the real and imaginary parts of the complex two-form parametrized by $\mathcal{C}$ as follows,

$$B_2 + iC_{(2)} = \mathcal{C}\,\mathrm{vol}_{\mathrm{S}^2} \ . \tag{4.2.16}$$

With the form of F in (4.2.3) we then have

$$\mathcal{F} = \mathfrak{F}\,\mathrm{vol}_{\mathrm{S}^2} \ , \qquad\qquad \mathfrak{F} = \mathcal{K} - \mathrm{Re}(\mathcal{C}) \ . \tag{4.2.17}$$

The sum in (4.2.5) therefore terminates at $n = 1$. From (4.2.15) we have

$$J^{(0)}_{(7)}\epsilon = -i\Gamma_{(0)}\epsilon \ , \qquad\qquad J^{(1)}_{(7)}\epsilon = -ie^{i\theta_\kappa}C\left(\Gamma_{(0)}\epsilon\right)^\star \ , \tag{4.2.18}$$

We have thus all the ingredients to explicitly evaluate the projection condition in (4.2.14). For the particular embedding where the D7-branes wrap $\mathrm{AdS}_6 \times \mathrm{S}^2$, we have

$$\Gamma_{(0)} = \Gamma_{01234567} \ , \tag{4.2.19}$$

where Γ_a are the ten-dimensional Clifford algebra generators, explicit indices $0, ..., 5$ are frame indices on AdS_6 and $6, 7$ are frame indices on S^2. Moreover,

$$\frac{1}{2}\gamma^{ij}X_{ij} = \gamma^{67}X_{67} = \Gamma^{67}\tilde{f}_2^{-2}\mathfrak{F} \ , \tag{4.2.20}$$

where, following the notation in [50], the tilde on f_2 denotes that it is the radius of S^2 in string frame. Finally,

$$\sqrt{\det(1+X)} = \sqrt{1+\tilde{f}_2^{-4}\mathfrak{F}^2} \ . \tag{4.2.21}$$

Using (4.2.19), (4.2.20), (4.2.21), as well as $C^2 = 1$ and $C\Gamma^a = (\Gamma^a)^\star C$, we find

$$\Gamma_\kappa\epsilon = \frac{-i}{\sqrt{\tilde{f}_2^4+\mathfrak{F}^2}}\Gamma_{01234567}\left(\tilde{f}_2^2\epsilon + e^{i\theta_\kappa}\mathfrak{F}\Gamma^{67}C^{-1}\epsilon^\star\right) \ . \tag{4.2.22}$$

Noting that raising all indices in $\Gamma_{01234567}$ produces a sign, and using (3.1.15), we thus find that the projection condition (4.2.14), after multiplying by $\sqrt{\tilde{f}_2^4+\mathfrak{F}^2}$, evaluates to

$$\sum_{\eta_1\eta_2}\chi^{\eta_1\eta_2}\otimes\left[\tilde{f}_2^2\zeta_{-\eta_1\,-\eta_2} + ie^{i\theta_\kappa}\mathfrak{F}\star\zeta_{-\eta_1\eta_2} - \sqrt{\tilde{f}_2^4+\mathfrak{F}^2}\zeta_{\eta_1\eta_2}\right] = 0 \ . \tag{4.2.23}$$

In order for the embedding to not break any supersymmetry, the term in square brackets has to vanish for all combinations of η_1 and η_2, and we thus arrive at

$$\tilde{f}_2^2 \zeta_{-\eta_1\,-\eta_2} + i e^{i\theta_\kappa} \mathfrak{F} \star \zeta_{-\eta_1\eta_2} - \sqrt{\tilde{f}_2^4 + \mathfrak{F}^2}\, \zeta_{\eta_1\eta_2} = 0 \ . \tag{4.2.24}$$

Using the explicit parametrization in (3.1.12), we immediately find that the conditions are not independent, but rather that imposing the equation to be satisfied for one combination of η_1 and η_2 implies the remaining conditions.

4.2.3 Solutions

To solve the BPS equations (4.2.23), we fix $\eta_1 = \eta_2 = +$. With the spinors ζ in (3.1.12) and $\star\zeta$ defined just above (3.1.12), the equation to solve becomes

$$\tilde{f}_2^2 \begin{pmatrix} -\bar{\alpha} \\ \beta \end{pmatrix} - i e^{i\theta_\kappa} \mathfrak{F} \begin{pmatrix} \bar{\beta} \\ \alpha \end{pmatrix} - \sqrt{\tilde{f}_2^4 + \mathfrak{F}^2} \begin{pmatrix} \bar{\alpha} \\ \beta \end{pmatrix} = 0 \ . \tag{4.2.25}$$

We note that setting $\mathfrak{F} = 0$ does not lead to consistent solutions unless $\alpha = 0$, and we therefore assume $\mathfrak{F} \neq 0$ from now on. Taking the complex conjugate of the second equation, the system we have to solve is

$$\begin{aligned} \left(\tilde{f}_2^2 + \sqrt{\tilde{f}_2^4 + \mathfrak{F}^2} \right) \bar{\alpha} + i e^{i\theta_\kappa} \mathfrak{F} \bar{\beta} = 0 \ , \\ \left(\tilde{f}_2^2 - \sqrt{\tilde{f}_2^4 + \mathfrak{F}^2} \right) \bar{\beta} + i e^{-i\theta_\kappa} \mathfrak{F} \bar{\alpha} = 0 \ . \end{aligned} \tag{4.2.26}$$

Multiplying the second equation by $(-i)e^{i\theta_\kappa}\mathfrak{F}^{-1}(\tilde{f}_2^2 + \sqrt{\tilde{f}_2^4 + \mathfrak{F}^2})$, which is manifestly non-zero if $\mathfrak{F} \neq 0$, reproduces the first equation. The two equations are thus not linearly independent and we are left with only one complex or two real conditions. From either of the two equations, and reality of $\tilde{f}_2$ and $\mathfrak{F}$, we conclude that $e^{-i\theta_\kappa}\bar{\alpha}/\bar{\beta}$ must be imaginary or, more

explicitly,

$$e^{i\vartheta} = \frac{\bar{\alpha}\beta}{\alpha\bar{\beta}} = -e^{2i\theta_\kappa} \ , \tag{4.2.27}$$

where we recognized the combination of Killing spinor components as the phase $e^{i\vartheta}$ introduced in sec. 4.3 of [48]. Eliminating the square root between the two equations in (4.2.26) yields

$$2\tilde{f}_2^2\bar{\alpha}\bar{\beta} + i\mathfrak{F}\left(e^{i\theta_k}\bar{\beta}^2 + e^{-i\theta_k}\bar{\alpha}^2\right) = 0 \ , \tag{4.2.28}$$

which is a real equation once (4.2.27) is satisfied. The BPS equations are thus (4.2.27), which determines the position of the D7 brane, and (4.2.28) which determines the flux as

$$\mathfrak{F} = \frac{2i\tilde{f}_2^2\bar{\alpha}\bar{\beta}}{e^{i\theta_k}\bar{\beta}^2 + e^{-i\theta_k}\bar{\alpha}^2} \ . \tag{4.2.29}$$

To evaluate the constraint on the position of the D7-brane in (4.2.27) more explicitly, we follow through the changes of variables in eq. (4.22) and (4.27) of [48]. This yields

$$e^{i\vartheta} = \frac{e^{i\psi} - \lambda R}{1 - e^{i\psi}\bar{\lambda}R} = \frac{\bar{\mathcal{L}} - \lambda\mathcal{L}R}{\mathcal{L} - \bar{\lambda}R\bar{\mathcal{L}}} \ , \tag{4.2.30}$$

where we used that $e^{i\psi} = \bar{\mathcal{L}}/\mathcal{L}$ (see (4.36) and (4.48) in [48]) to obtain the second equality. Finally, using $\kappa_-\bar{\mathcal{L}} = -\partial_w\mathcal{G}$ as well as $\kappa_\pm = \partial_w\mathcal{A}_\pm$ and $\lambda = \kappa_+/\kappa_-$ we can state the κ-symmetry condition (4.2.27) as

$$e^{i\vartheta} = \frac{\partial_{\bar{w}}\bar{\mathcal{A}}_-\partial_w\mathcal{G} - R\partial_w\mathcal{A}_+\partial_{\bar{w}}\mathcal{G}}{\partial_w\mathcal{A}_-\partial_{\bar{w}}\mathcal{G} - R\partial_{\bar{w}}\bar{\mathcal{A}}_+\partial_w\mathcal{G}} \stackrel{!}{=} -\frac{1+i\bar{\tau}}{1-i\tau} = -e^{2i\theta_\kappa} \ . \tag{4.2.31}$$

This is one real condition on the complex position of the D7-brane in Σ, and we thus expect a one-parameter family of solutions. We may evaluate this condition more explicitly by using

that, from the definition of B as $B = (1 + i\tau)/(1 - i\tau)$, we have

$$\frac{1 + i\bar{\tau}}{1 - i\tau} = \frac{1 + B}{1 + \bar{B}} \ . \tag{4.2.32}$$

The condition in (4.2.31) can thus be reformulated as

$$\left(\partial_{\bar{w}}\bar{\mathcal{A}}_{-}\partial_{w}\mathcal{G} - R\partial_{w}\mathcal{A}_{+}\partial_{\bar{w}}\mathcal{G}\right)(B+1) + \left(\partial_{w}\mathcal{A}_{-}\partial_{\bar{w}}\mathcal{G} - R\partial_{\bar{w}}\bar{\mathcal{A}}_{+}\partial_{w}\mathcal{G}\right)\left(\bar{B}+1\right) = 0 \ . \tag{4.2.33}$$

Using the definition of B in (3.1.9) as well as the explicit expressions for $\partial_w\mathcal{G}$ and $\partial_{\bar{w}}\mathcal{G}$ in terms of $\mathcal{A}_\pm$ and $\partial_w\mathcal{A}_\pm$ that follow from the definitions in (3.1.3), this evaluates to

$$(1+R)\kappa^2\left(\mathcal{A}_{+} + \bar{\mathcal{A}}_{+} - \mathcal{A}_{-} - \bar{\mathcal{A}}_{-}\right) = 0 \ . \tag{4.2.34}$$

Since $R \geq 0$ the first factor does not vanish. For $\kappa^2 \to 0$, the denominators in the original equation (4.2.31), by which we have multiplied, vanish, and a more careful treatment is needed. It shows that $\kappa^2 = 0$ is actually not a solution. This leaves the case where the combination of $\mathcal{A}_\pm$ and their conjugates in the last factor of (4.2.34) has to vanish. The latter condition, using $\bar{\mathcal{A}}^0_\pm = -\mathcal{A}^0_\mp$ and $\bar{Z}^\ell_\pm = -Z^\ell_\mp$, evaluates to

$$2\mathcal{A}^0_{+} - 2\mathcal{A}^0_{-} + \sum_{\ell=1}^{L}(Z^\ell_{+} - Z^\ell_{-})\ln|w - p_\ell|^2 = 0 \ . \tag{4.2.35}$$

This is our final form for the κ-symmetry condition restricting the position of the probe D7-brane.

4.2.4 Relation to backreacted solutions

The BPS condition for the probe D7-brane in (4.2.35) can be directly related to the regularity conditions for the warped AdS_6 solutions with monodromy in (4.1.3) and (4.1.4). The regularity conditions in (4.1.3) and (4.1.4) constrain the parameters for solutions with an

arbitrary number of punctures and relative weights n_i, and in particular also for the case that we consider one puncture with $n \equiv n_1$ infinitesimally small. To recover the probe analysis, we take the residues of the seed solution, $Z_\pm^\ell$, as given (with the constraint that they sum to zero) and determine the remaining parameters as formal power series in n from the regularity conditions. The ansatz for the parameters is

$$\begin{aligned} \mathcal{A}_\pm^0 &= \mathcal{A}_{\pm,0}^0 + n^2 \mathcal{A}_{\pm,2}^0 + \dots \ , & p_\ell &= p_{\ell,0} + n^2 p_{\ell,2} + \dots \ , \\ w_i &= w_{i,0} + n^2 w_{i,2} + \dots \ . \end{aligned} \tag{4.2.36}$$

At zeroth order in n, the conditions in (4.1.4) then reduce to the regularity conditions for a solution without monodromy, as given in (3.1.6). The conditions in (4.1.3), on the other hand, reduce precisely to the form of the κ-symmetry condition in (4.2.35). This independently supports the identification of the punctures with 7-branes.

4.3 S^5 partition function with backreacted 7-branes

In this section we turn to solutions with fully backreacted 7-branes and study the sphere partition functions of the dual SCFTs. We will focus on a class of 3-pole solutions and a class of 4-pole solutions. Implications for the relation to 5-brane webs will be discussed in sec. 4.4.

Since the SCFT is defined in odd dimensions, the renormalized sphere partition function is expected to be equal, up to a sign, to the finite part of the entanglement entropy for a ball-shaped region [34]. In chapter 3 we verified this relation explicitly for solutions without monodromy. In this chapter we take this relation for granted and we make use of it since the computation of the entanglement entropy is technically simpler. The derivation of section 3.3 can be straightforwardly applied to solutions without monodromy as well, we can use equations (3.3.3) and (3.3.4) which we report here for convenience:

$$S_{\rm EE} = \frac{1}{4G_{\rm N}} \, {\rm Vol}_{\rm S^2} \cdot \mathcal{J} \cdot {\rm Area}(\gamma_4) \tag{4.3.1}$$

$$\mathcal{J} = 4 \int_\Sigma d^2w f_6^4 f_2^2 \rho = \frac{8}{3} \int_\Sigma d^2w \; \kappa^2 \mathcal{G} = \frac{8}{3} \int_\Sigma d^2w (\partial_{\bar{w}} \mathcal{G}) \partial_w \mathcal{G} \ , \tag{4.3.2}$$

where

$$ {\rm Area}_{\rm ren}(\gamma_4) = \frac{2}{3} \, {\rm Vol}_{\rm S^3} \ . \tag{4.3.3}$$

Notice that we were able to integrate by parts straightforwardly because $\mathcal{G}$ and κ^2 are single valued. This saves an extra integration to obtain $\mathcal{G}$ and can thus be evaluated more efficiently.

The behavior of the entanglement entropy and thus the partition function under an overall rescaling of the charges can be obtained from a general scaling analysis, similar to the one carried out in section 3.2.1 for solutions without monodromy. The new aspect here of course is the presence of the punctures. From the explicit expression in (4.1.2), one can see that $\mathcal{A}_\pm$ transform homogeneously under the following rescaling of the charges

$$Z_\pm^\ell \to a Z_\pm^\ell \ , \qquad\qquad n_i \to n_i \ , \qquad\qquad a \in \mathbb{R} \ . \tag{4.3.4}$$

That is, the 5-brane charges are rescaled but the 7-brane monodromies are unchanged. The regularity conditions in (4.1.3), (4.1.4) are invariant if $\mathcal{A}_\pm^0 \to a \mathcal{A}_\pm^0$ with the p_ℓ and w_i unchanged. We thus find a solution again but with $\mathcal{A}_\pm \to a \mathcal{A}_\pm$. This implies $\partial_w \mathcal{G} \to a^2 \partial_w \mathcal{G}$ and thus

$$S_{\rm EE} \to |a|^4 S_{\rm EE} \ . \tag{4.3.5}$$

This scaling in particular holds for a ball-shaped region and therefore also applies for the sphere partition function. For the case of no punctures this reduces to the scaling derived in

3.2.1. The punctures therefore do not alter the scaling behavior, provided that they are not scaled with the 5-brane charges.

4.3.1 Dependence on branch cut orientation

From a brane-web picture interpretation we expect that the partition function does not depend on the location of the branch cut, i.e. we expect that if we continuously deform the branch cut, without crossing any poles, while keeping the physical charges of the external five-branes fixed, the partition function should be a constant.

This fact is far form obvious in our set up: the 5-brane charges, $\mathcal{Y}_+^\ell$, depend on the choice of the branch cut, so it is difficult to keep them fixed while deforming the branch cut. We take a slight different route and show that the invariance of the partition function is achieved by establishing two results. The first is that varying the orientation of the branch cut with fixed Z_+^ℓ does not change the partition function. Keeping Z_+^ℓ fixed while moving the branch cut induces a change in $\mathcal{Y}_+^\ell$. The second result shows that this change amounts to an overall $SL(2,\mathbb{R})$ transformation, which leaves the puncture and the 7-brane charge invariant. One may therefore compensate it with the inverse $SL(2,\mathbb{R})$ transformation, under which the partition function is, again, invariant. Together these results imply that the partition function is invariant under changes of the orientation of the branch cut with fixed charges of the external 5-branes, $\mathcal{Y}_+^\ell$.

To show that the partition function is invariant under changes of the branch cut orientation for fixed Z_+^ℓ, we set up an infinitesimal shift of one of the γ_i as follows,

$$\gamma_i \to \gamma_i(1 + i\delta\gamma) \ . \tag{4.3.6}$$

Since γ_i is a phase, $\delta\gamma$ is real. Under this change, we have

$$f(w) \to f(w) + \frac{in_i^2\delta\gamma}{4\pi} \ . \tag{4.3.7}$$

The locally holomorphic functions and their differentials transform as

$$\begin{aligned}\partial_w \mathcal{A}_\pm &\to \partial_w \mathcal{A}_\pm + \frac{in_i^2 \delta\gamma}{4\pi} \left(\partial_w \mathcal{A}_+ - \partial_w \mathcal{A}_-\right) \ , \\ \mathcal{A}_\pm &\to \mathcal{A}_\pm + \frac{in_i^2 \delta\gamma}{4\pi} \left(\mathcal{A}_+ - \mathcal{A}_-\right) \ . \end{aligned} \tag{4.3.8}$$

We furthermore notice that the $\mathcal{Y}_\pm^\ell$ change as follows,

$$\mathcal{Y}_\pm^\ell \to \mathcal{Y}_\pm^\ell + \frac{in_i^2 \delta\gamma}{4\pi} Y^\ell \ . \tag{4.3.9}$$

One can show that this new configuration still satisfies the regularity conditions (for details see [5]).

Equation (4.3.8) can be written as an $SL(2,\mathbb{R})$ transformation

$$\begin{aligned} \mathcal{A}_+ &\to u\mathcal{A}_+ - v\mathcal{A}_- \ , & u &= 1 + v \ , \\ \mathcal{A}_- &\to -\bar{v}\mathcal{A}_+ + \bar{u}\mathcal{A}_- \ , & v &= \frac{in_i^2 \delta\gamma}{4\pi} \ . \end{aligned} \tag{4.3.10}$$

Since $\mathcal{G}$ is invariant under $SL(2,\mathbb{R})$ transformations, and the same is true for $\partial_w \mathcal{G}$, the integrand in (4.3.2), which directly yields the partition function, is invariant under $SL(2,\mathbb{R})$. We have thus shown that the partition function is invariant under changes of the orientation of the branch cut with fixed Z_+^ℓ, as long as no poles are crossed.

Finally, we note that the transformation of the actual residues at the poles corresponding to the physical 5-brane charges, as given in (4.3.9), corresponds precisely to the $SL(2,\mathbb{R})$ transformation in (4.3.10). Performing the inverse $SL(2,\mathbb{R})$ transformation therefore yields a solution with unmodified $\mathcal{Y}_+^\ell$ but shifted orientation of the branch cut. In particular, the 7-brane charge is invariant under this $SL(2,\mathbb{R})$ transformation. The argument that the integrand in (4.3.2) is invariant under $SL(2,\mathbb{R})$ transformations again applies, and we have thus shown that the partition function is invariant under changes of the orientation of the branch cut, as long as no poles are crossed, while keeping the $\mathcal{Y}_+^\ell$ fixed.

4.3.2 3-pole solutions with D5, NS5 and D7

We now turn to explicit solutions and start with a class of 3-pole solutions discussed already in [74], where one of the external 5-brane stacks corresponds to D5 branes. The poles and overall normalization σ are chosen as

$$p_1 = 1 \ , \qquad p_2 = 0 \ , \qquad p_3 = -1 \ , \qquad \sigma = \frac{iN}{s_1} \ . \tag{4.3.11}$$

The regularity conditions in (4.1.3) and (4.1.4) are satisfied by the choices

$$\mathcal{A}^0_+ = iN \ln 2 + \frac{1}{2} J_1 \ , \qquad w_i = i\alpha_i \ , \quad \alpha_i \in \mathbb{R}^+ \ , \tag{4.3.12}$$

which in particular implies $J_1 = J_3$. This solves the regularity conditions for an arbitrary number of punctures, but we will focus on the case of a single puncture with D7-brane monodromy in the following. With $\alpha \equiv \alpha_1$ and $n \equiv n_1$ we thus have

$$f(w) = \frac{n^2}{4\pi} \ln\left(\gamma \frac{w - i\alpha}{w + i\alpha}\right) \ , \qquad \alpha \in \mathbb{R}^+ \ . \tag{4.3.13}$$

With $\mathfrak{s} = (s_1 - 1)/(2s_1)$, the residues are given by

$$\mathcal{Y}^1_+ = -iN \left[\mathfrak{s} + (\mathfrak{s} - \bar{\mathfrak{s}}) f(p_1)\right] \ , \quad \mathcal{Y}^2_+ = iN \ , \quad \mathcal{Y}^3_+ = iN \left[\mathfrak{s} - 1 + (\mathfrak{s} - \bar{\mathfrak{s}}) f(p_3)\right] \ . \tag{4.3.14}$$

That is, the pole p_2 corresponds to D5 branes, while the charges of the other two poles depend on the position of the puncture, the orientation of the branch cut and the remaining parameters.

We will solve for the parameters such that the residues take the form

$$\mathcal{Y}^1_+ = M \ , \qquad \mathcal{Y}^2_+ = iN \ , \qquad \mathcal{Y}^3_+ = -M \ . \tag{4.3.15}$$

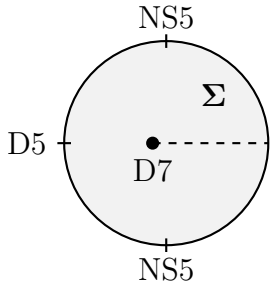

Figure 4.1: A disc representation of the 3-pole solution discussed in sec. 4.3.2

That is, a configuration with two poles corresponding to NS5 branes, one pole corresponding to D5 branes and one puncture corresponding to D7 branes. The setup is illustrated in fig. 4.1. This choice is obtained by imposing the following constraints:

$$\mathfrak{s} = im(1 - 2f(p_1)) \ , \qquad\qquad f(p_1) - f(p_3) = \frac{i}{2m} \ , \tag{4.3.16}$$

where $m = M/N$. The second equation gives one real constraint on the parameters associated with the puncture, n, α and γ.

Branch cut orientation

We now discuss the orientation of the branch cut in more detail. From sec. 4.3.1 we know that the partition function is independent of the choice of branch cut orientation as long as no poles are crossed. This still leaves the option for solutions with the same 5-brane and 7-brane charges, but which can not be deformed into each other without having a branch cut cross a pole.

Addressing this issue requires a careful treatment of the branch cuts, and to make that explicit we rewrite the constraint on the right hand side of (4.3.16) as follows

$$\int_{C(p_3,p_1)} dz\, \partial_z f(z) = \frac{i}{2m} \ , \qquad\qquad \partial_z f(z) = \frac{in^2}{4\pi} \frac{2\alpha}{z^2 + \alpha^2} \ , \tag{4.3.17}$$

where $C(p_3, p_1)$ denotes a contour from p_3 to p_1 that does not cross the branch cut in f. The

choice of contour depends on whether the branch cut in f intersects the boundary between p_1 and p_3 or not, and the choices are illustrated in fig. 4.2. If the branch cut does not intersect the boundary between p_1 and p_3, we can deform the contour to the segment of the real axis connecting p_3 to p_1 without crossing the puncture. If, on the other hand, the branch cut does intersect the boundary between p_1 and p_3, deforming the contour to the segment of the real axis between p_3 and p_1 picks up the residue at the pole $z = i\alpha$. We thus find the following constraint

$$\frac{i}{2m} = -2\pi i \delta_\gamma \mathrm{Res}_{z=i\alpha}(\partial_z f) + \int_{p_3}^{p_1} dx f'(x) \ , \tag{4.3.18}$$

where we defined $\delta_\gamma = 0$ if the branch cut does not intersect the boundary between p_3 and p_1, and $\delta_\gamma = 1$ if it does. Evaluating the residue and the integral along the real line yields

$$\frac{\pi}{2mn^2} = -\frac{\pi}{2}\delta_\gamma + \cot^{-1}\alpha \ . \tag{4.3.19}$$

The left hand side is positive, in view of the fact that $m > 0$ is required for $\mathrm{Im}(s_1) > 0$. The right hand side therefore has to be positive as well for a solution to exist. For $\alpha \in \mathbb{R}^+$, however, we have $0 < \cot^{-1}\alpha < \pi/2$. The right hand side is therefore negative if the branch cut intersects the boundary between p_1 and p_3, and the constraint can not be solved. The remaining option is to have the branch cut intersect the boundary outside of the interval (p_3, p_1), such that $\delta_\gamma = 0$. In that case a solution to the constraint exists provided that $mn^2 > 1$, and it is given by

$$\alpha = \cot\left(\frac{\pi}{2mn^2}\right) \ . \tag{4.3.20}$$

This solution is, in particular, independent of γ.

We thus find the following picture. Solving the regularity conditions for given 5-brane charge assignment, encoded by the $\mathcal{Y}^\ell_+$, and given 7-brane charge, encoded by n^2, imposes

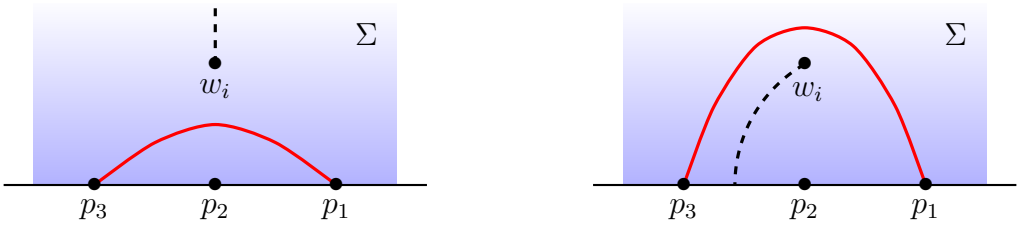

Figure 4.2: Integration contours for the constraint in (4.3.17), depending on whether or not the branch cut intersects the boundary in the interval (p_3, p_1).

a 'topological' constraint on the orientation of the branch cut. In the sense that it fixes between which poles the branch cut intersects the boundary, but not where exactly.

Fixed orientation of the branch cut

As shown in sec. 4.3.1, the partition function is invariant under changes in the orientation of the branch cut, as long as no poles are crossed, and as shown in the previous section the segment of the boundary in which the branch cut intersects intersects $\partial\Sigma$ is fixed. We now focus on the remaining dependence and keep the orientation of the branch cut, parametrized by γ, fixed. We choose it to extend in the positive imaginary direction, such that

$$\gamma = -1 \ , \qquad\qquad s_1 = \frac{i}{2m} \ . \tag{4.3.21}$$

This is compatible with the discussion in the previous section and the solution for α was given in (4.3.20).

As independent parameters we take M, N and n^2, while α is fixed by (4.3.20). To exhibit the functional dependence of the partition function, it is convenient to extract the overall scaling of the 5-brane charges. We analyze the partition function as a function of m, which is the ratio of NS5 and D5 charge, leaving N as the overall scale of the 5-brane charges, and

$$\mathfrak{n} = \frac{1}{mn^2} \ , \tag{4.3.22}$$

which is inspired by the form of α in (4.3.20). The dependence of the partition function on

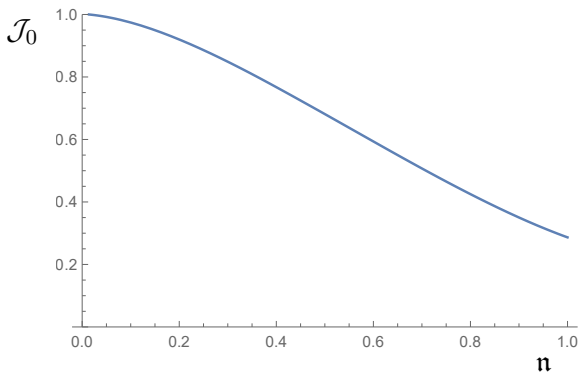

Figure 4.3: Plot of $\mathcal{J}_0$, which yields the partition function for the 3-pole solutions via (4.3.23).

the overall scale of the 5-brane charges, given by N, is quartic, as shown in (4.3.5). Since the location of the puncture depends on $\mathfrak{n}$ only, the combination $Y^\ell f(w)$, which appears in the definition of $\mathcal{A}_\pm$ and J_k, is independent of m. The $\mathcal{A}_\pm$ can therefore be split into an m-independent part and a part linear in m. Organizing the terms in $\mathcal{J}$ according to their m-scaling shows that only the linear part is non-vanishing, and we thus find that $\mathcal{J}$ is given by a function of $\mathfrak{n}$ multiplied by an overall factor of N^2M^2. Extracting also an overall numerical factor, we parametrize it as

$$\mathcal{J} = 224\pi\zeta(3)\, N^2M^2\mathcal{J}_0(\mathfrak{n})\ . \tag{4.3.23}$$

A plot of $\mathcal{J}_0(\mathfrak{n})$ is shown in fig. 4.3. The entanglement entropy for a ball shaped region, and thus the sphere partition function, is given by (3.3.5) with (4.3.3) and (4.3.23). The normalization in (4.3.23) is chosen such that $\mathcal{J}_0 = 1$ reproduces the partition function of a four-pole solution without monodromy, corresponding to an intersection of D5 and NS5 branes, as discussed in [4].

4.3.3 Turning a puncture into a pole

We now discuss how a 4-pole solution with D5 and NS5 branes can be recovered from the 3-pole solutions with D5 and NS5 branes and a puncture. To this end, we start from the

configuration with fixed orientation of the branch cut, as discussed in sec. 4.3.2. Recall that we have three poles at

$$p_1 = 1 \ , \qquad p_2 = 0 \ , \qquad p_3 = -1 \ , \tag{4.3.24}$$

with residues given by

$$\mathcal{Y}^1_+ = M \ , \qquad \mathcal{Y}^2_+ = iN \ , \qquad \mathcal{Y}^3_+ = -M \ . \tag{4.3.25}$$

These residues could be realized by choosing the orientation of the branch cut as $\gamma = -1$, and the position of the branch cut α related to the number of 7-branes at the puncture, parametrized by n^2, as in (4.3.20), such that

$$f(w) = \frac{n^2}{4\pi} \ln\left(\frac{i\alpha - w}{i\alpha + w}\right) \ , \qquad \alpha = \cot\left(\frac{\pi}{2mn^2}\right) \ . \tag{4.3.26}$$

We will consider this family of solutions as parametrized by the location of the branch point, α, and study the limit $\alpha \to \infty$. The relation on the right hand side in (4.3.26) can be solved straightforwardly for n^2 and we can then expand for large α, which yields

$$n^2 = \frac{\pi\alpha}{2m} + \mathcal{O}(\alpha^{-1}) \ , \qquad f(w) = \frac{iw}{4m} + \mathcal{O}(\alpha^{-1}) \ . \tag{4.3.27}$$

In particular, to realize a family of solution with fixed $\mathcal{Y}^\ell_+$ as given in (4.3.25), the number of D7-branes at the puncture has to grow with α as the puncture is moved towards infinity (which is a regular point of the boundary of the disc). Due to this growing behavior, the function f remains non-trivial in the limit.

We will now show that, as $\alpha \to \infty$, the differentials $\partial_w \mathcal{A}_\pm$ approach those of a 4-pole solution, with the three poles on the boundary of Σ that were present already for finite α, and an extra pole at infinity. The general form of the differentials for a solution with

monodromy can be obtained straightforwardly from (4.1.2), which yields

$$\partial_w \mathcal{A}_\pm = \sum_{\ell=1}^{L} \frac{Z_\pm^\ell}{w-p_\ell} + f(w) \sum_{\ell=1}^{L} \frac{Y^\ell}{w-p_\ell} \ . \tag{4.3.28}$$

With the limiting behavior of f in (4.3.27) and expressing $Z_\pm^\ell$ in terms of $\mathcal{Y}_\pm^\ell$ using the definition in (4.1.6), we find

$$\partial_w \mathcal{A}_\pm\big|_{\alpha\to\infty} = \sum_{\ell=1}^{L} \frac{1}{w-p_\ell} \left(\mathcal{Y}_\pm^\ell - f(p_\ell) Y^\ell\right) + \frac{iw}{4m} \sum_{\ell=1}^{L} \frac{Y^\ell}{w-p_\ell} \ . \tag{4.3.29}$$

For the particular family of solutions we are considering here, we have $Y^2 = 0$ and $Y^1 = -Y^3$. Straightforward evaluation then shows that the terms proportional to Y^ℓ cancel and the differentials reduce to

$$\partial_w \mathcal{A}_\pm\big|_{\alpha\to\infty} = \sum_{\ell=1}^{L} \frac{\mathcal{Y}_\pm^\ell}{w-p_\ell} \ . \tag{4.3.30}$$

That is, the differentials for a solution with poles at (4.3.24) with residues given in (4.3.25). However, since the sum over $\mathcal{Y}_\pm^\ell$ does not vanish, we also have a pole at infinity, with residue given by[1]

$$\mathcal{Y}_\pm^4\big|_{\alpha\to\infty} = -\sum_{\ell=1}^{3} \mathcal{Y}_\pm^\ell = -iN \ . \tag{4.3.31}$$

We can thus explain the limiting behavior of the partition function computed in sec. 4.3.2: As $\alpha \to \infty$, we have $\mathfrak{n} \to 0$. As explained below (4.3.23), the partition function of a four-pole solution with D5 and NS5 poles with residues iN and M, respectively, is recovered from (4.3.23) for $\mathcal{J}_0 = 1$. From fig. 4.3 we indeed see that

$$\lim_{\mathfrak{n}\to 0} \mathcal{J}_0(\mathfrak{n}) = 1 \ , \tag{4.3.32}$$

[1]Solutions without monodromy and a pole at infinity have been discussed in more detail in [4].

as we expect from the fact the the three-pole solution with puncture reduces to a four-pole solution without puncture in that limit.

4.4 Implications for the brane web picture

As discussed in more detail in [49, 50], the AdS_6 solutions without monodromy have a compelling interpretation as supergravity description of 5-brane intersections. This clear interpretation is facilitated by the very natural mapping between the parameters of the supergravity solutions and the parameters fixing a 5-brane intersection: once the charges of the external 5-branes are fixed, supersymmetry completely fixes an intersection, and correspondingly a supergravity solution. With the introduction of punctures into the supergravity solutions and 7-branes into the 5-brane picture, this mapping of parameters becomes more involved. While there is still a clear relation of the supergravity parameters to the brane charges in the string theory picture (the 7-brane charge is given directly by n^2 while the physical 5-brane charges are given by the $\mathcal{Y}^{\ell}_{\pm}$ via (4.1.7)), the process of engineering a supergravity solution that realizes a given set of charges is more complicated. Moreover, a general analysis of the number of parameters alone is not sufficient anymore to completely specify the map between supergravity solution and brane webs.

The partition functions of the dual SCFTs may be used to discriminate different interpretations for the parameters of the supergravity solutions, since the partition functions are expected to agree for solutions that describe physically equivalent brane webs which realize the same SCFT. In the following we will discuss the mapping of parameters between supergravity solutions and brane webs, and the results on the partition functions in that context. As shown in [74], the number of free parameters for a solution with L poles and I punctures is given by

$$2L - 2 + 3I \ . \tag{4.4.1}$$

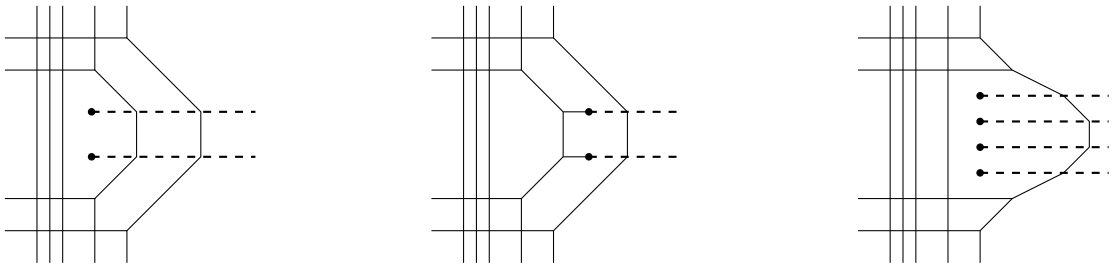

(a) (b) (c)

Figure 4.4: Fig. 4.4(a) shows a possible 5-brane web corresponding to the class of supergravity solutions illustrated in fig. 4.1, with a puncture corresponding to two D7 branes. The brane web shows a general deformation of the SCFT, not the fixed point. Fig. 4.4(b) and 4.4(c) show two options for 5-brane webs with the same external 5-brane charges but 7-branes in a different face of the web. The web in fig. 4.4(b) is related to the web in fig. 4.4(a) by 7-brane moves, the web in fig. 4.4(c) is not.

$2L-2$ parameters naturally arise as a choice of residues, Z_+^ℓ, *of a seed solution*, subject to the constraint that they sum to zero. The three extra parameters per puncture correspond to the 7-brane charge, the location of the branch point on a curve in Σ, and the orientation of the branch cut. While the charge and orientation of the branch cut have a clear interpretation in the brane web picture, the freedom to choose a location on Σ may seem puzzling. A crucial point for the interpretation of the solutions is that, upon adding punctures, the residues at the poles are modified and given by the $\mathcal{Y}_\pm^\ell$ in (4.1.6) instead of $Z_\pm^\ell$, and that it is these modified residues that correspond to physical 5-brane charges. To address the interpretation of the parameters associated with the puncture, we have for that reason realized families of configurations with fixed $\mathcal{Y}_\pm^\ell$ in sec. 4.3.2.

In sec. 4.3.2 we discussed the case of two NS5 brane poles, one D5 brane pole and one puncture. For fixed orientation of the branch cut *and* fixed $\mathcal{Y}_\pm^\ell$, we found a two-parameter family of solutions, where the 7-brane charge n^2 and the location of the puncture parametrized by α are related as given in (4.3.20), and the remaining parameter is the orientation of the branch cut. Fixing a complete set of 5-brane and 7-brane charges therefore entirely fixes the configuration, up to the choice of branch cut orientation. Upon varying the position of the puncture one may keep either the 5-brane charges or the 7-brane charge

fixed, but not both. This picture is consistent with the parameter count in (4.4.1) as follows. In the presence of 7-branes, the D5-brane charge is not necessarily conserved at the intersection. Fixing the 5-brane charges given by $\mathcal{Y}^{\ell}_{\pm}$ in the presence of punctures therefore fixes $2L-1$ parameters, instead of $2L-2$. For one puncture that leaves two free parameters, corresponding to the 7-brane charge and the orientation of the branch cut. For the case of more than one puncture, we expect relative motions of the punctures as free parameters.

To better understand the remaining parameters for one puncture, we analyzed the sphere partition function. At fixed 5-brane and 7-brane charges, we found that the partition function does not depend on infinitesimal changes in the branch cut orientation – at least as long as no poles are crossed. This is indeed consistent with the brane web picture: changing the orientation of the branch cut in the example web shown in fig. 4.4(a), without crossing any external 5-branes, changes the web, which describes a deformation of the SCFT. But it does not change the conformal limit, in which the web collapses to an intersection at a point. This would indeed suggest that the partition function of the UV fixed point, which is the theory described by the supergravity solution, should be independent of the precise orientation of the branch cut as long as it does not cross poles, precisely as we found in sec. 4.3.2.

The results on the partition function also allow for conclusions on the interpretation of the position of the puncture. We assume that the location of the puncture on Σ corresponds to which face of the web the 7-branes are located in, which naturally becomes a continuous parameter in the "large-N" limit: with large numbers of external 5-branes, one finds a dense grid of faces, and the choice of which face the 7-branes are placed in remains meaningful in the conformal limit. One may then consider two options for supergravity solutions with the same 5-brane charges but a puncture at different positions:

(i) They are related by literally moving 7-branes within the web, with the corresponding Hanany-Witten brane creation of 5-brane prongs stretching between the 7-branes and the 5-branes of the web.

(ii) They correspond to genuinely different brane webs, where the 7-branes are placed

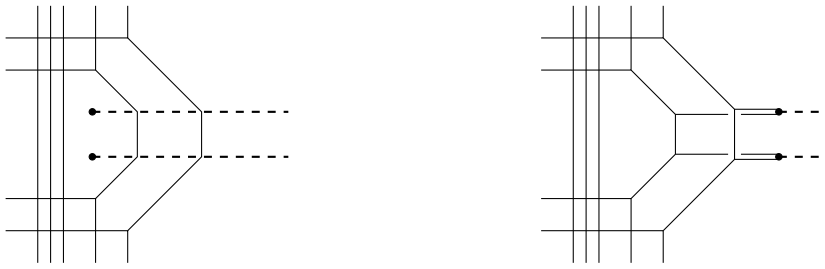

Figure 4.5: Starting from the web shown in fig. 4.4(a) and moving the 7-branes out of the web along their branch cuts produces 5-brane prongs stretching between the 7-branes and the 5-branes of the web, with avoided intersections due to the s-rule shown as broken lines.

in different faces, without 5-brane prongs stretching between the 7-branes and the 5-branes.

The two options are illustrated for a particular choice of 5-brane web in fig. 4.4. In case (i), one would expect the 7-brane charge to not vary as the location of the puncture is changed while keeping the external 5-brane charges fixed, as is clearly borne out by fig. 4.4(b). The field theory would remain unchanged as the location of the puncture is changed, and the same would be expected for the S^5 partition function of the SCFT described by the web. In case (ii), one would expect the 7-brane charge that is required to keep the external 5-brane charges fixed to vary as the location of the puncture is varied, as is exhibited in fig. 4.4(c). The webs would describe genuinely different SCFTs and the partition functions would be expected to differ. As we found in sec. 4.3.2, the charge has to be related to the location of the branch cut in a non-trivial way, as is given in (4.3.20), to preserve the external 5-brane charges. Moreover, the dependence of the partition function on the remaining free parameter is non-trivial, as can be seen explicitly from the plot in fig. 4.3. Both of these results are inconsistent with case (i), but are very well in line with option (ii). Our results show that solutions with the same 5-brane charges but punctures at different points in Σ describe genuinely different brane webs and dual SCFTs, and the webs in fig. 4.4(a) and 4.4(c) appear as natural brane web realizations of the solutions.

The parametrization of $\mathcal{J}$, which yields the entanglement entropy for a ball shaped

region or equivalently the sphere partition function via (3.3.5), was chosen in (4.3.23) such that $\mathcal{J}_0 = 1$ reproduces the partition function for a 4-pole solution with D5-brane poles and NS5-brane poles with residues M and iN, respectively, as computed in [4]. One might expect that a solution with 3 poles and a puncture is related to a solution with 4 poles and no puncture via Hanany-Witten transitions: pulling the D7-brane out of the 5-brane web produces a D5 brane whenever an NS5 brane is crossed, and one may suspect to get back to a solution with no puncture but an extra pole in this way. This was described in detail for an $SU(2)$ web in [41]. However, for brane webs with large N and M, and a D7 brane in a generic face of the web, we do not expect such a relation. The reason is illustrated in fig. 4.5: due to the s-rule [62, 75], which states that no two D5 branes ending on the same 7-brane can end on the same NS5 brane while preserving supersymmetry, one would create avoided intersections in the process of pulling the D7 branes out of the web. These avoided intersections remain even if the D7-branes are moved off to infinity, and this process does therefore not lead back to a pure 5-brane web. This explains why the partition functions for the supergravity solutions computed in sec. 4.3.2 do in general not agree with that of a 4-pole solution without puncture.

However, as discussed in sec. 4.3.3, we can recover a 4-pole solution without monodromy by moving the puncture along its branch cut towards the boundary of Σ, while scaling up the 7-brane charge such that the physical 5-brane charges remain invariant. This limiting procedure can be interpreted in the brane web picture as follows. For a given 7-brane we can define the notion of a distance to the "boundary of the web" as the number of 5-branes that cross its branch cut. For example, for the 7-branes shown in fig. 4.4(a), this distance is 2. The limit discussed in sec. 4.3.3 can then be interpreted as increasing the number of D7-branes while placing them in faces such that their distance to the "boundary of the web" decreases. The transition from the web in fig. 4.4(a) to the web in fig. 4.4(c) gives an example of one step in this limit. The external 5-brane charges are the same for the two webs, but the distance to the "boundary of the web" is decreased from 2 to 1 in going from 4.4(a) to 4.4(c),

Figure 4.6: Starting from the web shown in fig. 4.4(c), where the branch cut of each 7-brane is crossed by only one 5-brane, and moving the 7-branes out of the web, produces a pure 5-brane web with no avoided intersections. Vertically aligning the D7-branes in the web on the right hand side with the external D5 branes turns the web into an intersection of D5 and NS5 branes. This deformation corresponds to a change of the flavor masses; the conformal UV fixed point, which is described by the supergravity solution, remains the same.

while the number of D7 branes is doubled. For a supergravity solution with a puncture at a generic point on Σ, the distance to the "boundary of the web" of the corresponding 7-branes will be a generic number greater than one. But as the puncture is moved along its branch cut towards the boundary of Σ, this number decreases, until the 7-branes are eventually separated from the asymptotic region by only one 5-brane. Crossing this remaining 5-brane then produces 5-branes via the Hanany-Witten effect, with no constraints from the s-rule and no avoided intersections. For the web in fig. 4.4(c) this step is shown in fig. 4.6. The 7-branes may now be moved off to infinity and we recover a pure 5-brane intersection. In this particular case that is an intersection of D5 and NS5 branes. This gives a brane web explanation for the fact that the partition function of a 3-pole solution with puncture agrees with the partition function of a 4-pole solution without puncture in the limit of sec. 4.3.3.

Bibliography

[1] A. Trivella, "Holographic Computations of the Quantum Information Metric," *Class. Quant. Grav.* **34** (2017), no. 10 105003, 1607.06519.

[2] D. Bak and A. Trivella, "Quantum Information Metric on $\mathbb{R} \times S^{d-1}$," *JHEP* **09** (2017) 086, 1707.05366.

[3] M. Gutperle and A. Trivella, "Note on entanglement entropy and regularization in holographic interface theories," *Phys. Rev.* **D95** (2017), no. 6 066009, 1611.07595.

[4] M. Gutperle, C. Marasinou, A. Trivella, and C. F. Uhlemann, "Entanglement entropy vs. free energy in IIB supergravity duals for 5d SCFTs," *JHEP* **09** (2017) 125, 1705.01561.

[5] M. Gutperle, A. Trivella, and C. F. Uhlemann, "Type IIB 7-branes in warped AdS_6: partition functions, brane webs and probe limit," *JHEP* **04** (2018) 135, 1802.07274.

[6] L. Amico, R. Fazio, A. Osterloh, and V. Vedral, "Entanglement in many-body systems," *Rev. Mod. Phys.* **80** (May, 2008) 517–576.

[7] S. Ryu and T. Takayanagi, "Holographic derivation of entanglement entropy from AdS/CFT," *Phys. Rev. Lett.* **96** (2006) 181602, hep-th/0603001.

[8] J. Bhattacharya, V. E. Hubeny, M. Rangamani, and T. Takayanagi, "Entanglement density and gravitational thermodynamics," *Phys. Rev.* **D91** (2015), no. 10 106009, 1412.5472.

[9] T. Faulkner, M. Guica, T. Hartman, R. C. Myers, and M. Van Raamsdonk, "Gravitation from Entanglement in Holographic CFTs," *JHEP* **03** (2014) 051, 1312.7856.

[10] N. Lashkari, C. Rabideau, P. Sabella-Garnier, and M. Van Raamsdonk, "Inviolable energy conditions from entanglement inequalities," *JHEP* **06** (2015) 067, 1412.3514.

[11] M. Miyaji, T. Numasawa, N. Shiba, T. Takayanagi, and K. Watanabe, "Distance between Quantum States and Gauge-Gravity Duality," *Phys. Rev. Lett.* **115** (2015), no. 26 261602, 1507.07555.

[12] D. Bak, "Information metric and Euclidean Janus correspondence," *Phys. Lett.* **B756** (2016) 200–204, 1512.04735.

[13] D. Bak, M. Gutperle, and S. Hirano, "A Dilatonic deformation of AdS(5) and its field theory dual," *JHEP* **05** (2003) 072, hep-th/0304129.

[14] S.-J. Gu, "Fidelity Approach to Quantum Phase Transitions," *Int. J. Mod. Phys. B* **24** (2010) 4371, 0811.3127.

[15] K. Skenderis, "Lecture notes on holographic renormalization," *Class. Quant. Grav.* **19** (2002) 5849–5876, hep-th/0209067.

[16] D. Bak, A. Gustavsson, and S.-J. Rey, "Conformal Janus on Euclidean Sphere," *JHEP* **12** (2016) 025, 1605.00857.

[17] C. Fefferman and C. R. Graham, "Conformal invariants," in *Élie Cartan et les mathématiques d'aujourd'hui - Lyon, 25-29 juin 1984*, no. S131 in Astérisque, pp. 95–116. Société mathématique de France, 1985.

[18] T. Takayanagi, "Holographic Dual of BCFT," *Phys. Rev. Lett.* **107** (2011) 101602, 1105.5165.

[19] M. Fujita, T. Takayanagi, and E. Tonni, "Aspects of AdS/BCFT," *JHEP* **11** (2011) 043, 1108.5152.

[20] O. Aharony, O. DeWolfe, D. Z. Freedman, and A. Karch, "Defect conformal field theory and locally localized gravity," *JHEP* **07** (2003) 030, hep-th/0303249.

[21] A. Karch and L. Randall, "Open and closed string interpretation of SUSY CFT's on branes with boundaries," *JHEP* **06** (2001) 063, hep-th/0105132.

[22] J. Estes, K. Jensen, A. O'Bannon, E. Tsatis, and T. Wrase, "On Holographic Defect Entropy," *JHEP* **05** (2014) 084, 1403.6475.

[23] S. A. Gentle, M. Gutperle, and C. Marasinou, "Entanglement entropy of Wilson surfaces from bubbling geometries in M-theory," *JHEP* **08** (2015) 019, 1506.00052.

[24] S. A. Gentle, M. Gutperle, and C. Marasinou, "Holographic entanglement entropy of surface defects," *JHEP* **04** (2016) 067, 1512.04953.

[25] M. Srednicki, "Entropy and area," *Phys. Rev. Lett.* **71** (1993) 666–669, hep-th/9303048.

[26] K. Jensen and A. O'Bannon, "Holography, Entanglement Entropy, and Conformal Field Theories with Boundaries or Defects," *Phys. Rev.* **D88** (2013), no. 10 106006, 1309.4523.

[27] E. D'Hoker, J. Estes, and M. Gutperle, "Exact half-BPS Type IIB interface solutions. II. Flux solutions and multi-Janus," *JHEP* **06** (2007) 022, 0705.0024.

[28] E. D'Hoker, J. Estes, and M. Gutperle, "Interface Yang-Mills, supersymmetry, and Janus," *Nucl. Phys.* **B753** (2006) 16–41, hep-th/0603013.

[29] E. D'Hoker, J. Estes, and M. Gutperle, "Exact half-BPS Type IIB interface solutions. I. Local solution and supersymmetric Janus," *JHEP* **06** (2007) 021, 0705.0022.

[30] E. D'Hoker, J. Estes, M. Gutperle, and D. Krym, "Janus solutions in M-theory," *JHEP* **06** (2009) 018, 0904.3313.

[31] M. Nozaki, T. Takayanagi, and T. Ugajin, "Central Charges for BCFTs and Holography," *JHEP* **06** (2012) 066, 1205.1573.

[32] K. Jensen and A. O'Bannon, "Constraint on Defect and Boundary Renormalization Group Flows," *Phys. Rev. Lett.* **116** (2016), no. 9 091601, 1509.02160.

[33] J. Brown and M. Henneaux, "Central charges in the canonical realization of asymptotic symmetries: An example from three dimensional gravity," *Commun.Math. Phys.* **104** (1986), no. 2 207–226.

[34] H. Casini, M. Huerta, and R. C. Myers, "Towards a derivation of holographic entanglement entropy," *JHEP* **05** (2011) 036, 1102.0440.

[35] W. Nahm, "Supersymmetries and their Representations," *Nucl. Phys.* **B135** (1978) 149.

[36] V. G. Kac, "Lie Superalgebras," *Adv. Math.* **26** (1977) 8–96.

[37] N. Seiberg, "Five-dimensional SUSY field theories, nontrivial fixed points and string dynamics," *Phys. Lett.* **B388** (1996) 753–760, hep-th/9608111.

[38] K. A. Intriligator, D. R. Morrison, and N. Seiberg, "Five-dimensional supersymmetric gauge theories and degenerations of Calabi-Yau spaces," *Nucl. Phys.* **B497** (1997) 56–100, hep-th/9702198.

[39] O. Aharony and A. Hanany, "Branes, superpotentials and superconformal fixed points," *Nucl. Phys.* **B504** (1997) 239–271, hep-th/9704170.

[40] O. Aharony, A. Hanany, and B. Kol, "Webs of (p,q) five-branes, five-dimensional field theories and grid diagrams," *JHEP* **01** (1998) 002, hep-th/9710116.

[41] O. DeWolfe, A. Hanany, A. Iqbal, and E. Katz, "Five-branes, seven-branes and five-dimensional E(n) field theories," *JHEP* **03** (1999) 006, hep-th/9902179.

[42] A. Brandhuber and Y. Oz, "The D-4 - D-8 brane system and five-dimensional fixed points," *Phys. Lett.* **B460** (1999) 307–312, hep-th/9905148.

[43] O. Bergman and D. Rodriguez-Gomez, "5d quivers and their AdS(6) duals," *JHEP* **07** (2012) 171, 1206.3503.

[44] D. L. Jafferis and S. S. Pufu, "Exact results for five-dimensional superconformal field theories with gravity duals," *JHEP* **05** (2014) 032, 1207.4359.

[45] B. Assel, J. Estes, and M. Yamazaki, "Wilson Loops in 5d N=1 SCFTs and AdS/CFT," *Annales Henri Poincare* **15** (2014) 589–632, 1212.1202.

[46] L. F. Alday, M. Fluder, P. Richmond, and J. Sparks, "Gravity Dual of Supersymmetric Gauge Theories on a Squashed Five-Sphere," *Phys. Rev. Lett.* **113** (2014), no. 14 141601, 1404.1925.

[47] L. F. Alday, M. Fluder, C. M. Gregory, P. Richmond, and J. Sparks, "Supersymmetric gauge theories on squashed five-spheres and their gravity duals," *JHEP* **09** (2014) 067, 1405.7194.

[48] E. D'Hoker, M. Gutperle, A. Karch, and C. F. Uhlemann, "Warped $AdS_6 \times S^2$ in Type IIB supergravity I: Local solutions," *JHEP* **08** (2016) 046, 1606.01254.

[49] E. D'Hoker, M. Gutperle, and C. F. Uhlemann, "Holographic duals for five-dimensional superconformal quantum field theories," *Phys. Rev. Lett.* **118** (2017), no. 10 101601, 1611.09411.

[50] E. D'Hoker, M. Gutperle, and C. F. Uhlemann, "Warped $AdS_6 \times S^2$ in Type IIB supergravity II: Global solutions and five-brane webs," 1703.08186.

[51] Y. Lozano, E. Ó Colgáin, D. Rodríguez-Gómez, and K. Sfetsos, "Supersymmetric AdS_6 via T Duality," *Phys. Rev. Lett.* **110** (2013), no. 23 231601, 1212.1043.

[52] Y. Lozano, E. Ó Colgáin, and D. Rodríguez-Gómez, "Hints of 5d Fixed Point Theories from Non-Abelian T-duality," *JHEP* **05** (2014) 009, 1311.4842.

[53] F. Apruzzi, M. Fazzi, A. Passias, D. Rosa, and A. Tomasiello, "AdS_6 solutions of type II supergravity," *JHEP* **11** (2014) 099, 1406.0852. [Erratum: JHEP05,012(2015)].

[54] H. Kim, N. Kim, and M. Suh, "Supersymmetric AdS_6 Solutions of Type IIB Supergravity," *Eur. Phys. J.* **C75** (2015), no. 10 484, 1506.05480.

[55] H. Kim and N. Kim, "Comments on the symmetry of AdS_6 solutions in String/M-theory and Killing spinor equations," 1604.07987.

[56] J. B. Gutowski and G. Papadopoulos, "On supersymmetric AdS6 solutions in 10 and 11 dimensions," 1702.06048.

[57] J. H. Schwarz, "Covariant Field Equations of Chiral N=2 D=10 Supergravity," *Nucl. Phys.* **B226** (1983) 269.

[58] P. S. Howe and P. C. West, "The Complete N=2, D=10 Supergravity," *Nucl. Phys.* **B238** (1984) 181–220.

[59] J. X. Lu and S. Roy, "An SL(2,Z) multiplet of type IIB super five-branes," *Phys. Lett.* **B428** (1998) 289–296, hep-th/9802080.

[60] D. Corbino, E. D'Hoker, and C. F. Uhlemann, "$AdS_2 \times S^6$ versus $AdS_6 \times S^2$ in Type IIB supergravity," 1712.04463.

[61] T. Okuda and D. Trancanelli, "Spectral curves, emergent geometry, and bubbling solutions for Wilson loops," *JHEP* **09** (2008) 050, 0806.4191.

[62] F. Benini, S. Benvenuti, and Y. Tachikawa, "Webs of five-branes and N=2 superconformal field theories," *JHEP* **09** (2009) 052, 0906.0359.

[63] C. R. Graham and E. Witten, "Conformal anomaly of submanifold observables in AdS / CFT correspondence," *Nucl. Phys.* **B546** (1999) 52–64, hep-th/9901021.

[64] O. Bergman, D. Rodríguez-Gómez, and G. Zafrir, "Discrete θ and the 5d superconformal index," *JHEP* **01** (2014) 079, 1310.2150.

[65] L. Bao, V. Mitev, E. Pomoni, M. Taki, and F. Yagi, "Non-Lagrangian Theories from Brane Junctions," *JHEP* **01** (2014) 175, 1310.3841.

[66] H. Hayashi, H.-C. Kim, and T. Nishinaka, "Topological strings and 5d T_N partition functions," *JHEP* **06** (2014) 014, 1310.3854.

[67] M. Taki, "Notes on Enhancement of Flavor Symmetry and 5d Superconformal Index," 1310.7509.

[68] M. Taki, "Seiberg Duality, 5d SCFTs and Nekrasov Partition Functions," 1401.7200.

[69] M. Fluder and C. F. Uhlemann, "Precision Test of AdS_6/CFT_5 in Type IIB String Theory," *Phys. Rev. Lett.* **121** (2018), no. 17 171603, 1806.08374.

[70] O. Bergman and G. Zafrir, "Lifting 4d dualities to 5d," *JHEP* **04** (2015) 141, 1410.2806.

[71] S.-S. Kim, M. Taki, and F. Yagi, "Tao Probing the End of the World," *PTEP* **2015** (2015), no. 8 083B02, 1504.03672.

[72] H. Hayashi, S.-S. Kim, K. Lee, M. Taki, and F. Yagi, "A new 5d description of 6d D-type minimal conformal matter," *JHEP* **08** (2015) 097, 1505.04439.

[73] H. Hayashi, S.-S. Kim, K. Lee, and F. Yagi, "6d SCFTs, 5d Dualities and Tao Web Diagrams," 1509.03300.

[74] E. D'Hoker, M. Gutperle, and C. F. Uhlemann, "Warped $AdS_6 \times S^2$ in Type IIB supergravity III: Global solutions with seven-branes," *JHEP* **11** (2017) 200, 1706.00433.

[75] A. Hanany and E. Witten, "Type IIB superstrings, BPS monopoles, and three-dimensional gauge dynamics," *Nucl. Phys.* **B492** (1997) 152–190, hep-th/9611230.

[76] E. Bergshoeff and P. Townsend, "Super D-branes," *Nucl.Phys.* **B490** (1997) 145–162, hep-th/9611173.

[77] M. Cederwall, A. von Gussich, B. E. Nilsson, and A. Westerberg, "The Dirichlet super three-brane in ten-dimensional type IIB supergravity," *Nucl.Phys.* **B490** (1997) 163–178, hep-th/9610148.

[78] M. Cederwall, A. von Gussich, B. E. Nilsson, P. Sundell, and A. Westerberg, "The Dirichlet super p-branes in ten-dimensional type IIA and IIB supergravity," *Nucl.Phys.* **B490** (1997) 179–201, hep-th/9611159.

[79] A. Karch, B. Robinson, and C. F. Uhlemann, "Supersymmetric D3/D7 for holographic flavors on curved space," *JHEP* **11** (2015) 112, 1508.06996.

[80] M. Grana and J. Polchinski, "Gauge / gravity duals with holomorphic dilaton," *Phys. Rev.* **D65** (2002) 126005, hep-th/0106014.